Scuola Internazionale Superiore Studi Avanzati

International School for Advanced Studies

Joint PhD Program in Molecular Biology

Trieste, Italy

Functional and Molecular Impact of *Foxg1* Over-expression in Neocortical Projection Neurons

Thesis submitted for the degree of “Doctor Philosophiae”

Academic Year 2018/2019

Candidate:

Wendalina Tigani

Supervisor:

Prof. Antonello Mallamaci

Abstract

Foxg1 is an evolutionary conserved transcription factor gene playing a crucial role in a variety of neurodevelopmental processes taking place in the rostral brain. Mice overexpressing *Foxg1* in their neocortical projection neurons were previously generated and characterized in our laboratory. These mice showed an increased activity in baseline conditions and a higher incidence of limbic motor seizures upon kainic acid administration (Tigani, Pinzan et al., submitted).

In this study we modulated *Foxg1* gene expression in primary cultures of neocortical neurons to model its impact on activity of neocortical pyramids.

We evaluated neuronal activity through Ca^{2+} imaging assay and found that the over-expression of our gene of interest led to hyperactivity and hyper-synchronization of the culture. Interestingly, neuronal hyperactivity was also achieved when the up-regulation of our gene was limited to glutamatergic cells.

Given this, we wondered whether GABAergic neurons were affected by *Foxg1* over-expression. We observed a pronounced depletion of GABAergic interneurons, indeed, when the genetic manipulation occurred in the whole neuronal compartment of the culture.

Aiming to dissect molecular mechanisms leading to *Foxg1*-dependent neuronal hyperactivity, we profiled the transcriptome of *Foxg1*-GOF neurons and detected a misregulation of a number of key genes, encoding for crucial players such as ion channels, GABA and glutamate receptors.

We also detected a transient *Foxg1* up-regulation presumably ignited by neuronal activity, upon the administration of KCl. We monitored the response to the same treatment of some immediate early genes and found that they are necessary to *Foxg1* mRNA increase and contribute to its early articulation.

Taken all together, these data suggest that even small changes of *Foxg1* levels result in a deep impact on pyramids' activity, an issue relevant to neuronal physiology and neurological aberrancies associated to *FOXG1* copy number variations.

Contents

1. Introduction

1.1 Neocortex development

The development of nervous system begins at the trilaminar embryo, the stage following gastrulation in which the embryo has a structure consisting of the 3 germ cell layers: ectoderm, mesoderm, and endoderm. The ectoderm forms the outer epithelium of the body (epidermis) and the neural plate, from which the nervous system develops. Folding along its central axis the neural plate forms a neural groove lined on each side by a neural fold. The fusion of the neural folds generates the neural tube, that will give rise to the three primary brain vesicles, namely the forebrain vesicle (prosencephalon), the midbrain vesicle (mesencephalon), and the hindbrain vesicle (the rhombencephalon). The embryonic forebrain can be divided morphologically and functionally into the telencephalon diencephalon, hypothalamus and retinae. The telencephalon consists in the cerebral cortex, basal ganglia and olfactory bulb. In higher mammals, the largest region of the cerebral cortex is the neocortex (phylo-genetically its most recent component), positioned between the archicortex (midline cortex and hippocampus) and paleocortex (piriform cortex) [1].

The sequence of events of telencephalic development is similar in mammals, although with different timings. In the mouse, at the beginning of the second half of gestation, the telencephalic vesicles consist in two dorsolateral expansions of the primary forebrain vesicle. When the telencephalic vesicles bulge from the prosencephalon, they comprise only germinal neuroepithelium that will give rise to the six-layered cerebral cortex. The first step in lamination of the dorsal telencephalic wall is its division into an inner layer of proliferating cells, called the ventricular zone (VZ), and an outer layer known as the preplate or primordial plexiform layer (PPL) [2,3]. Proliferating cells residing in the early VZ, namely the forerunners of the majority of neurons and glial cells of the cerebral cortex, give rise to the pseudostratified ventricular epithelium (PVE), roughly corresponding to later VZ itself, and the secondary proliferative population (SPP), approximately corresponding to the subventricular zone (SVZ). PPL is conversely formed by the earliest born neurons. Later, the PPL is penetrated by later born neurons, which split it into a superficial marginal zone (MZ), forerunner of neocortex layer I, and a deep subplate (SP), fated to subsequently disappear and get incorporated in deep neocortical layer VI. Such later born neurons

accumulate in between MZ and SP and form the so-called cortical plate (CP), precursor of neocortical layers VI-II, where they settle according to the canonical inside-out rule (the earlier born the deeper, the later born the more superficial). Following the cessation of neuronal production there is a massive production of astrocytes and oligodendrocytes, which continues postnatally. Neurogenesis in the mouse neocortex occurs from embryonic day 12-17 [4], while gliogenesis occurs later (Fig. 1).

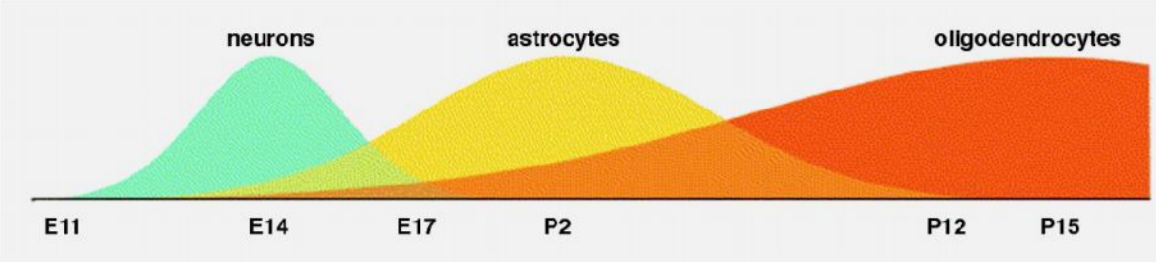

Figure 1. Murine cortico-cerebral histogenesis.

After the dramatic tangential expansion of the neocortical field occurring between E10 and E12, around E13-E14, the neocortical VZ increases in width, due to cells of the PVE dividing rapidly to increase the size of the population of progenitors. At E14-E16 SPP consists only of 11% of the total proliferative population. At E15 the VZ has reached its maximum thickness and then declines by the end of E16. In the E15-E16 interval the number of SPP cells increases more than twice, while PVE cells are almost halved. In contrast to the reduction in width of the VZ and corresponding dramatic reduction in cell numbers in the PVE, the rest of the cortical strata (molecular layer, cortical plate, intermediate zone and SVZ) increase in width through E16. The subplate starts to decrease in width and is eventually lost. By E17 the PVE disappears while the proliferative activity of the SPP continues postnatally and eventually becomes confined to the subependymal layer. By E18/E19 the thickness of the overlying intermediate zone/white matter and developing cortical plate are at their maximum widths. All neuronal cells have exited the cell cycle and have migrated to their final position within the developing cortex.

Neocortical precursors

As anticipated above, in rodents two distinct proliferative populations mainly arise from the primordial VZ: the pseudostratified ventricular epithelium (PVE) and the secondary proliferative population (SPP). These two cell types differ in their distributions within the cell wall and in their proliferative behavior too. The PVE lies adjacent to the ventricle and is present since the outset of the cerebral hemispheres' evagination. This population is composed by earlier neuroepithelial cells and later radial glial cells, both undergoing interkinetic nuclear migration and "serving" as stem cells from which the vast majority of mature neural types of neocortex will derive. The SPP is a highly heterogeneous proliferating population, including first neuronogenic and then astrogenic committed progenitors. They differ from stem cells, because, during cell cycle progression, their nucleus typically does not give rise to radial oscillations peculiar to the former ones[5]. Initially, a single sheet of pseudostratified neuroepithelial cells undergoes both symmetric cell divisions, to expand the pool of multipotent progenitors, as well as asymmetric cell divisions, to generate the earliest born neurons[6–8]. As neurogenesis progresses, neuroepithelial cells transform into radial glia [9,10], known to have crucial roles in guiding neurons to their final locations in the cortical plate by serving as a migratory scaffolding [11,12]. A further role of radial glia was proposed by recent studies, showing that at least some of these cells also function as progenitors and generate pyramidal neurons either directly through mitoses at the apical surface of the VZ, or indirectly through the production of intermediate progenitors [9,10,13–17]. Intermediate progenitors generate deep-layer and upper-layer projection neurons, under the influence of specific genes. The role of the most important genes involved in the specification of neocortical progenitors will be deepened in the next paragraph.

Specification of neocortical progenitors

Upon induction of the telencephalon a number of genes that direct neocortical neurogenesis are expressed across the dorsolateral wall of the telencephalon. These include Lhx2 (LIM homeobox 2), Foxg1 (forkhead box G1), Emx2 (empty spiracles homologue 2) and Pax6 (paired box 6). Each of them is crucial in specifying the progenitors that will originate the projection neurons of the neocortex. Thanks to these four genes, the neocortical progenitor domain is established by repressing dorsal midline (Lhx2 and Foxg1) and ventral (Emx2 and Pax6) fates. Emx2 and Pax6, expressed in opposite and overlapping gradients in the dorsal telencephalon, are key determinants

of the proper development of cortical areas[18] and are also required for establishing the identity of dorsal progenitors[19]. Loss of both empty spiracles homologue 2 (Emx2) and paired box 6 (Pax6) results in ventralization of cortical progenitors and the loss of the neocortical domain (Ncx), archicortex (Acx), cortical hem (CH) and choroid plexus (CPl) by embryonic day 14[19]. Pax6, along with Nr2e1, also controls the proliferation of VZ progenitors during the establishment and expansion of the SVZ [20–22]. Loss of LIM homeobox 2 (Lhx2) results in the expansion of the CPl and CH medial domains and the elimination of progenitors with neocortical identity. Similarly, loss of forkhead box G1 (Foxg1) causes agenesis of the basal ganglia, elimination of neocortical progenitor domains and expansion of the CH and the Acx [23] (Fig. 2).

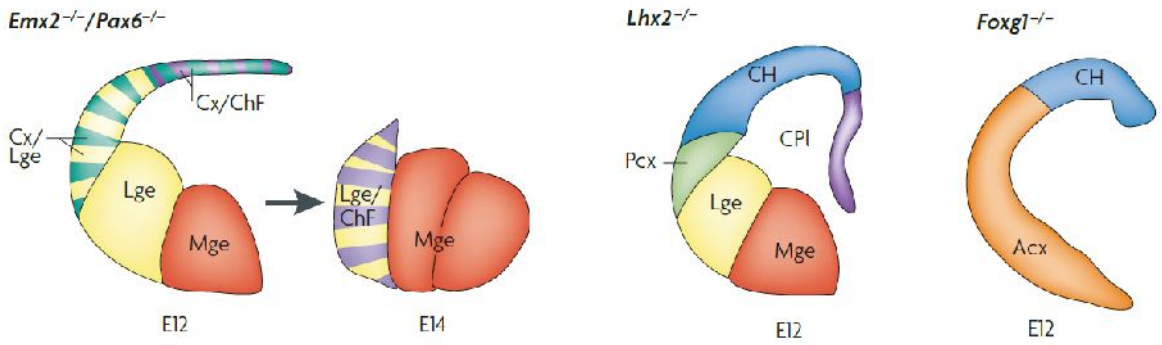

Fig. 2. Crucial roles of Emx2, Pax6, Lhx2 and Foxg1 in the specification of neocortical progenitors. Ncx, neocortex; Acx, archicortex; Cx, cortex; CH, cortical hem; CPI, choroid plexus; CR, choroidal roof; ChF, choroid field (choroid plexus and choroidal roof); Lge, lateral ganglionic eminence; Mge, medialganglionic eminence; Pcx, paleocortex. Adapted from Molyneaux et al. 2007 [23].

Origin and migration of glutamatergic and gabaergic neurons

We can distinguish cortical neurons into two broad classes. On one hand interneurons, that make local connections. On the other projection neurons, which extend axons to distant intracortical, subcortical and subcerebral targets[23]. Projection neurons are glutamatergic and prevalently characterized by a typical pyramidal morphology. During development, they are generated from progenitors of the neocortical germinal zone located in the dorsolateral wall of the telencephalon [11,24–27] and migrate radially toward the cortical plate. During their radial migration, phases of temporary migratory arrest and others of retrograde migration were observed prior to entering the

CP [28]. During these phases, migrating neurons transition between bipolar and multipolar morphologies [29]. Migration of pyramidal neurons will be further described ahead in this chapter, with a particular focus on the role of Foxg1 on this process.

By contrast, GABAergic interneurons are generated primarily from progenitors in the ventral telencephalon. They migrate long distances to their final locations within the neocortex [30]. Upon arrival, interneurons move radially to enter the CP [31]. They then segregate into their layer destinations depending on their molecular subtype, origin and birth date during early postnatal development [32]. In this way, different progenitor zones contribute to the variety of neuronal types in the neocortex.

Projection neuron specification

Born in the germinal zone, projection neurons migrate to the cortical plate, where they extend a primary axon generally pointing towards the ventricular side of the cortical wall. This axon may further project towards other ispilateral or heterolateral cortical areas (layer II-III and layer V cortico-cortical projection neurons). Alternatively, navigating via the internal capsule, it may point to the thalamus (layer VI cortico-thalamic projecting neurons) or, via cerebral peduncle and pyramidal tract, to brainstem and spinal cord (layer Vb cortico-subthalamic projection neurons). Secondary collaterals sprout from the axon after it passed other targets[33]. Inappropriate connections are later eliminated, leaving subcerebral projection neurons in the sensorimotor cortex projecting to the caudal pons and spinal cord, whereas those in the visual cortex maintain projections to the rostral pons and superior colliculus[33–35]. Given this common pattern of initial development, several genes regulating early specification and differentiation are likely to be shared amongst different types of subcerebral projection neurons [36].

Fezf2, a putative transcription factor that is expressed in all subcerebral projection neurons from early stages of development through adulthood [36,37], was recently found to be required for the specification of all sub-cerebral projection neurons. In the absence of Fezf2 function in null mutant mice, the entire population of subcerebral projection neurons is absent, and there are no projections from the cerebral cortex to either the spinal cord or the brainstem. Fezf2 does not seem to affect the ability of progenitors to generate glutamatergic neurons that position themselves in layer V; it probably acts to direct the next step in the programme of specification. Consistently,

overexpression of Fezf2 resulted sufficient to induce the birth of entirely new deep-layer projection neurons[38,39].

Ctip2 was identified as a crucial regulator of subcerebral axon extension. In the absence of Ctip2, subcerebral projection neuron axons exhibit defects in fasciculation, outgrowth and pathfinding, with decreased numbers of axons reaching the brainstem[36].

Another key transcription factor known to have a role in the target choice of subcerebral projection neurons is Otx1. This protein is expressed in putative deep-layer progenitors in the VZ, exhibiting decreasing levels of expression in the VZ during the generation of upper-layer neurons [37,40]. Otx1-/-mice show defects in the development of corticotectal projection neurons. Otx1 might have a later role in subcerebral projection neuron development than Fezf2 and Ctip2, perhaps by controlling the refinement and pruning of axonal collaterals.

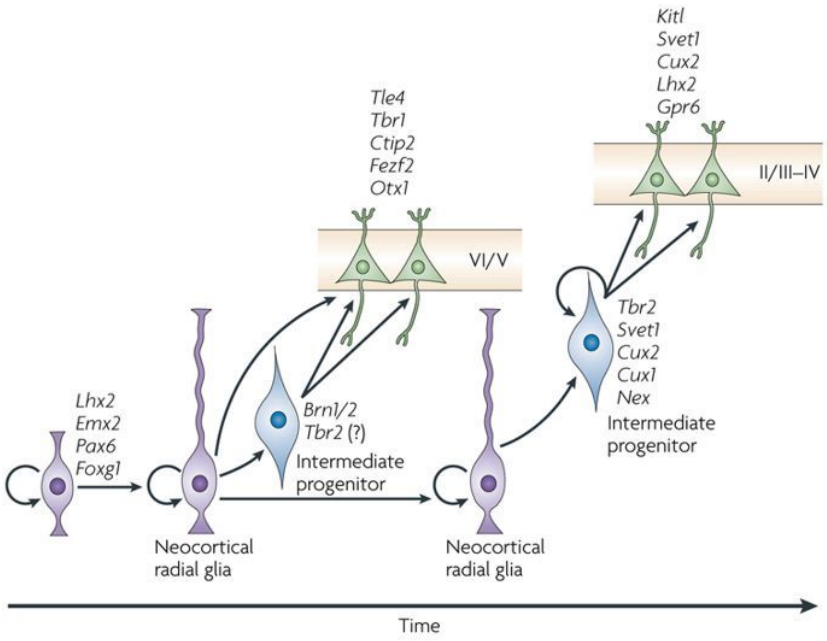

Figure 3. Schematic representation of a potential model for the generation of projection neuron subtypes from progenitors. Adapted from Molyneaux et al. 2007 [23].

A possible model for the generation of subcerebral projection neurons is described in figure 3. Briefly, the concerted function of Foxg1, Lhx2, Pax6 and Emx2 first gives progenitors neocortical potential, allowing the generation of multiple classes of glutamatergic projection neurons. Radial glial progenitors could express a series of transcription factors. These are maintained in

intermediate progenitors and post mitotic neurons, imparting subtype identity. Thus, during the generation of subcerebral projection neurons, genes such as Brn1 and Brn2 might act on partially specified progenitors to determine aspects of laminar identity as individual subtypes of pyramidal neurons are generated. Fezf2 could then specify the subcerebral projection neuron lineage within a layer (layer V), enabling the development of the molecular, morphological and anatomical projection properties of subcerebral projection neurons. Finally, the expression of genes such as Ctip2 and Otx1, which govern subcerebral axonal outgrowth and target selection, could act to establish the precise connectivity and later morphological features of subcerebral projection neurons. Further works identified several laminar- and subtype-specific markers[41–44] expanding the number of known layer- and subtype-specific genes (reviewed in figure 4), thus suggesting further candidate effectors implicated in layer-specific differentiation programs. As for laminar specification, this is still controversial. The existence of early dedicated precursors selectively able to generate deep layer (VI-V) or upper layer (IV-II) projection neurons was reported [45], however this finding was later questioned and it was shown that Fezf2^{+} precursors within the very early VZ can generate both upper and deep layer neurons [46].

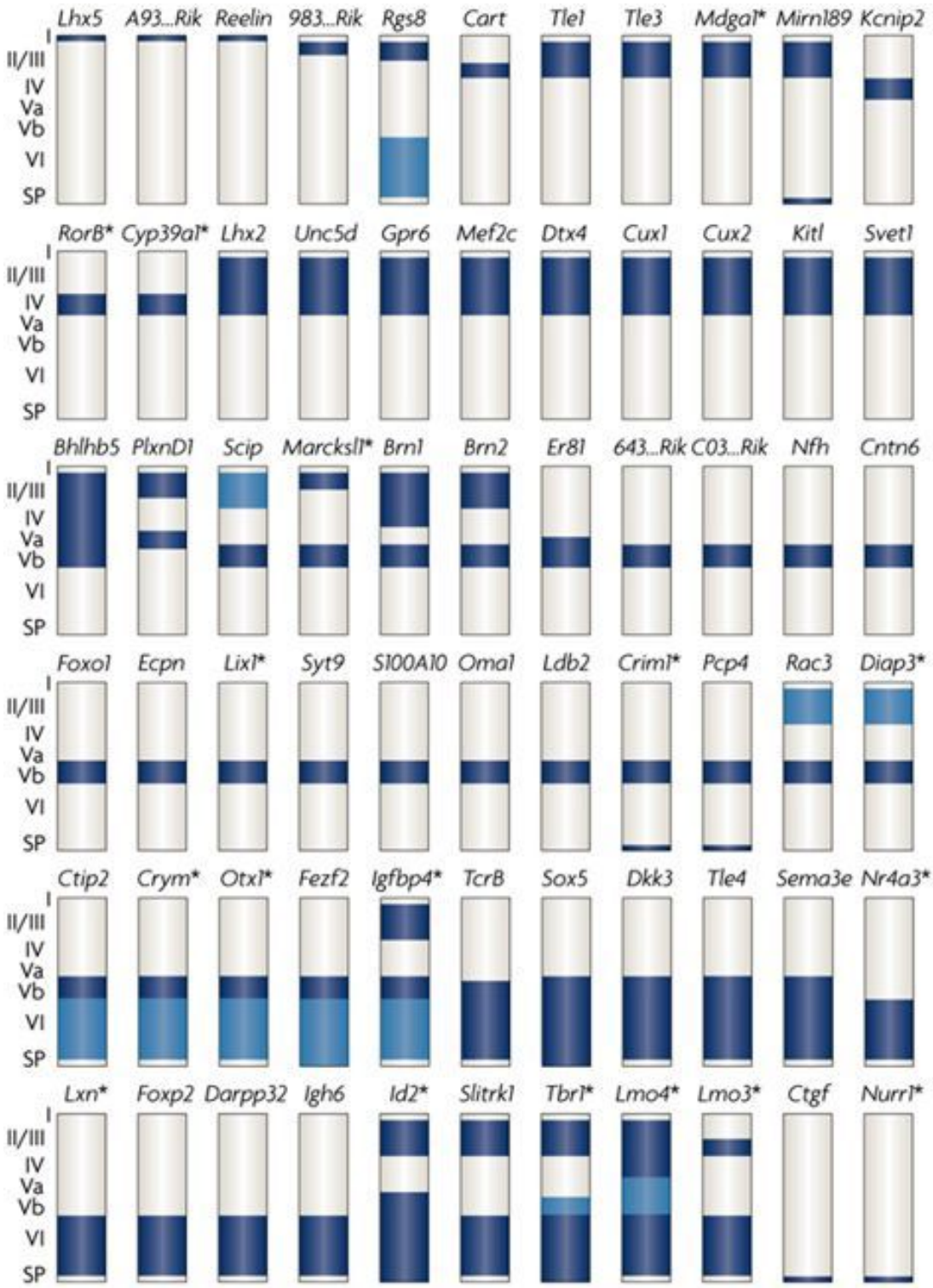

Figure 4. Schematic of cortical layers depicting the laminar-specific expression of 66 genes within the neocortex. Dark blue and light blue indicate higher and lower relative levels of expression, respectively. Genes for which laminar or subtype expression varies by area within the neocortex are indicated by an asterisk. Adapted from Molyneaux et al. 2007 [23].

Astrocytes

Astrocytes are the largest glial population in the mammalian brain[47]. They provide structural support, modulate the chemical environment by influencing water balance and ion distribution, and participate in the blood-brain barrier maintenance. Astrocytes are also crucial for the development of neural circuits and provide support to the dynamic machinery underlying synapse formation, function and elimination. Indeed, they regulate calcium flux and also release and reuptake neuropeptides [48,49].They are commonly classified in three main types, according to morphology and spatial organization: radial astrocytes surrounding ventricles, protoplasmic astrocytes in grey matter and fibrous astrocytes in white matter [50]. Astrocytes are generated later than neurons from the same pool of neural stem cells (NSCs) in the gliogenic phase of late gestation (Fig. 1). During development (in mouse E9-10) NSCs start to display radial processes, becoming radial glial cells (RG) (Fig 5).

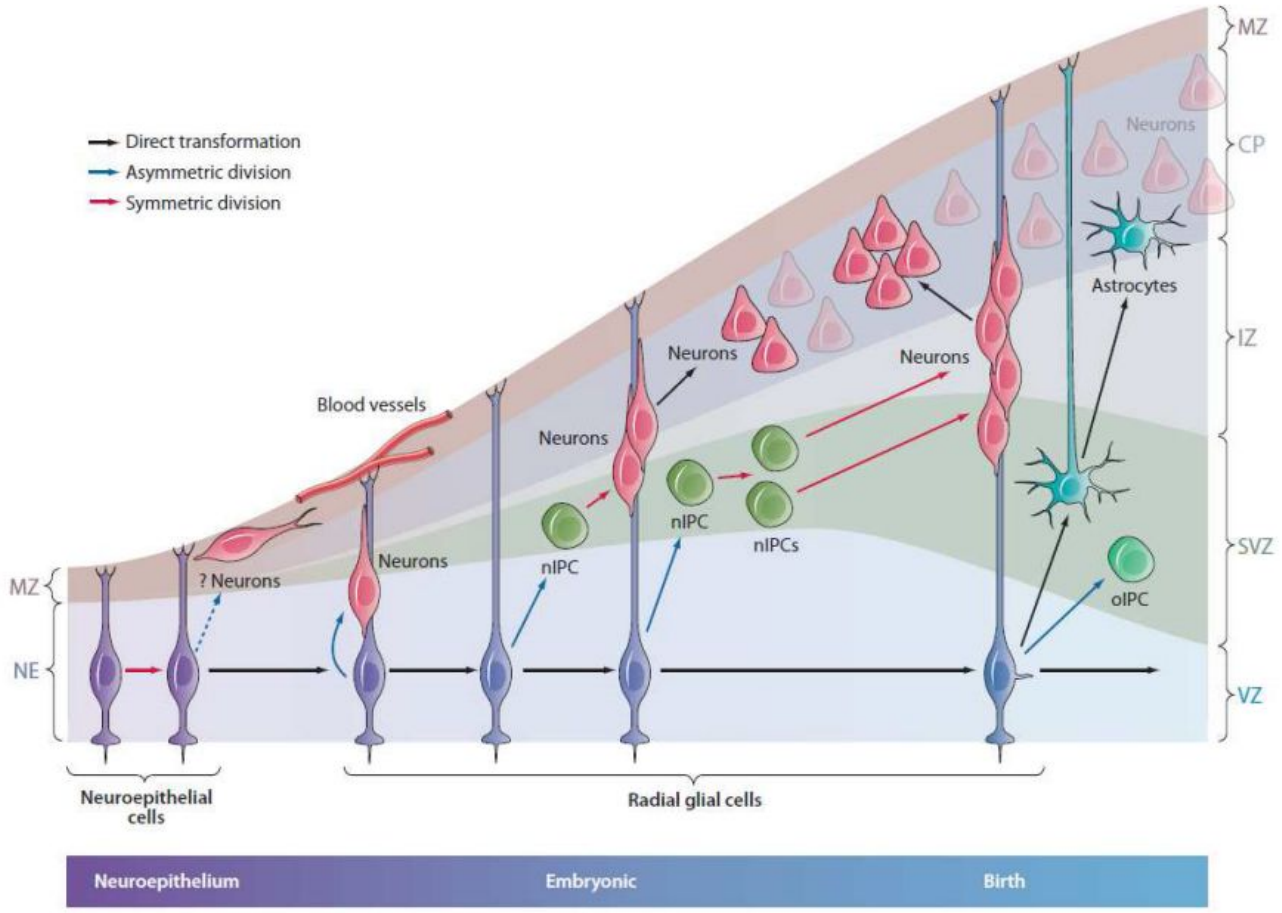

Figure 5. Neurogenesis during cortical development (adapted from Kriegstein and Alvarez-Buylla 2009 [51])

RG have contacts with both pial and ventricular surfaces, but cell bodies within the VZ. The lengthening of the pia-directed radial process is associated with the progressive thickening of the cortex throughout neurogenesis. RG show proliferative activity, can directly give rise to neurons, or, more frequently, to different pools of intermediate progenitors. A second output of dorsal telencephalic RG cells is represented by astrocytes, which are generated largely after the neuronogenic process is completed.

Most astrocytes, still divide locally before terminal differentiation[52]. A peak in the production of astrocytes just after birth is reported, then this phenomenon globally fades around the end of the second week of postnatal life. Nevertheless, the process of astrocytic proliferation may as well be detected in the postnatal murine cortex [53,54].

1.2 Neuronal Excitability

The key mechanism of neuronal excitability is the action potential. It occurs in an all-or-none fashion because of local depolarization of the membrane. The membrane depolarization is propagated down the axon to induce neurotransmitter release at the axon terminal. The membrane potential varies through different processes: the activation of ligand-gated channels, whose conductance changes when binding to neurotransmitters; or the activation of voltage-gated channels, whose conductance changes with the transmembrane potential. Neurotransmitters are released by the axon terminal into the synaptic cleft, next they bind specific postsynaptic receptors. Ligand binding lead to channel activation and flow of ions into or out of the postsynaptic cells. The major neurotransmitters in the brain are glutamate, gamma-amino-butyric acid (GABA), acetylcholine (ACh), norepinephrine, dopamine, serotonin, and histamine. Other factors such as neuropeptides and hormones play modulatory roles that modify neurotransmission over longer time periods [55].

The main excitatory neurotransmitter is the amino acid glutamate. There are several subtypes of glutamate receptors: alpha-amino-2,3-dihydro-5-methyl-3-oxo-4-isoxazolepropanoic acid (AMPA), kainate receptors, and N-methyl-D-aspartate (NMDA). They differ from one another by cation permeability as well as differential sensitivity to drugs. The influx of Na+ and outflow of K^+ through these channels mainly contribute to the generation of the action potential. The other major type of glutamate receptor is the metabotropic one, which functions by means of receptor-activated signal transduction involving membrane-associated G-proteins [56].

The main inhibitory neurotransmitter is GABA. This molecule interacts with two major receptors: GABAA, found post-synaptically, and GABAB, which is found pre-synaptically and can thereby modulate synaptic release. In the adult brain GABAA receptors are permeable to Cl^- ions. When the receptors are activated the Cl^- influx hyperpolarizes the membrane, inhibiting the action potentials. The GABAB receptors are instead associated with second messenger systems rather than Cl^- channels. They lead to the attenuation of the transmitter release due to their presynaptic location. The second messenger systems often result in the opening of K^+ channels, leading to a hyperpolarizing current [57].

Mechanisms governing excitability of single neurons may act inside the neuron or in the cellular environment, including other cells as well as the extracellular space. Examples of "intrinsic" factors might be the type, number and distribution of voltage- and ligand-gated channels, biochemical modification of receptors, activation of second-messenger systems, RNA editing of channels. Among "extrinsic" factors are reported: variations in extracellular ion concentration, remodeling of synapsis, modified metabolism or uptake of neurotransmitters by astrocytes [55].

Of note, glial cells in this context play a crucial role in regulating the environment surrounding neurons. Astrocytes, indeed, buffer extracellular potassium released by firing neurons and remove glutamate from the extracellular space, stopping its excitatory effect at the level of the synapsis. Besides, astrocytes can release glutamate as well. In this way they modulate synaptic activity in nearby neurons increasing their excitability and promoting synchrony of neuronal action potential firing [58,59].

In this scenario, it is also important to take into account that neurons connect together in a complex network, providing additional levels of control. Thus, changes in the function of one or more cells within a circuit can significantly affect both neighboring and distant neurons.

Given all this, a hyper excitable condition might arise from several mechanism: an increase in excitatory synaptic neurotransmission, decreased inhibitory neurotransmission, alteration in voltage-gated ion channels, or variations of intra- or extra-cellular ion concentrations in favor of membrane depolarization. Of note, also several synchronous subthreshold excitatory stimuli can bring to a hyper excitable state. Disrupting the mechanisms that inhibit firing or promoting the mechanisms that facilitate excitation alters the physiological balance of excitation and inhibition. This leads to seizures, the clinical manifestation of excessive and hypersynchronous discharge [60].

1.3 Forkhead box G1 transcription factor

Forkhead box G1 (Foxg1) is an ancient, evolutionary conserved transcription factor gene. It belongs to the forkhead box family and it plays a crucial role in patterning, morphogenesis, cell differentiation and proliferation. The key feature of FOX proteins is the so-called fork-head box DNA binding domain. It consists of 80-100 aminoacidic residues, forming three N-terminal alpha-helices, three beta-strands and two loops [61]. Located in human chromosome 14q.13 and mouse chr.12q.B3, *Foxg1* is one of the first TF genes expressed in the developing rostral brain and is fundamental for the correct development of telencephalon. It is involved in cerebral cortex morphogenesis, in dorsoventral patterning of the pallium, cell cycle control, lineage fate choices induction, regulation of neocortical cell differentiation and migration, tuning of astrogenesis rates. Most of these roles will be described in this chapter.

Of note, it was broadly shown that even subtle alterations in its expression result in defects in the brain development or pathological conditions grouped as *Foxg1* syndromes. Further information about this condition will be provided in a dedicated paragraph.

Foxg1 and telencephalic induction

Foxg1 takes part to a complex network of signaling pathways both promoting ventral identity and limiting the dorsal territory via a direct Wnt ligands' repression.

Starting from E7 in mice, the primitive node and the anterior visceral endoderm (AVE) send signals for neural induction and maintenance in order to organize the early rostro-caudal patterning [62]. Cerberus and Dickkopf proteins, secreted by AVE, repress the posteriorizing effect of molecules expressed by the neural plate, such as Wnt, Fgfs family members and retinoic acid (RA) [63,64].

Following anterior neural induction, the Anterior Neural Ridge (ANR) promotes telencephalic development triggering the expression of *Foxg1* via Fgf8 secretion [65,66]. An important role in inducing *Foxg1* expression is exerted by Hedgehog signaling [67]. Thus, the coordinated stimulation by Fgf8 from ANR and Shh from the prechordal plate, generates a gradient of *Foxg1* expression: high levels ventral/anterior area, decreasing toward dorsal/posterior zone.

The dorso/ventral specification of telencephalon is orchestrated by a balance of Gli3 and Shh expression, showing dorsalizing and ventralizing effects, respectively [68,69]. In this context, Foxg1 cooperates with Fgf as ventralizing signal, in order to generate ventral cell types [70]. Notably, Foxg1 also inhibits dorsal fates by limiting Wnt expression, directly binding to Wnt8b promoter [67]. As a consequence of that, ablation of *Foxg1* resulted in a strong impairment of the subpallium [71], full abortion of neocortical and paleocortical programs [72], an enlargement of the hippocampal anlage and a dramatic excess of Cajal Retzius neurons production [72,73]. Foxg1/Gli3 double mutants have an enlarged, unpaired, rostromedial vescicle with mixed telencephalic-diencephalic identity, suggesting an earlier and more fundamental role of these factors in specification of the telencephalic vs diencephalic anlage [74].

Foxg1 in neural precursors kinetics

Another pivotal role of our gene of interest is exerted in the regulation of the balance between proliferation and differentiation of neural precursors. During corticogenesis, these cells give rise to all the cell populating the cortex. At this level, the control of cell cycle progression and governing is crucial. During neurogenesis, indeed, cell cycle duration is progressively prolonged, thanks to the lengthening of the G1 phase. In addition, an increasing number of cells exit from cell cycle[75] and cells start undergoing asymmetrical differentiate divisions, instead of selfrenewing symmetrical ones [6,76]. These processes are finely regulated by Cdk-Cyclin complex inhibitors of the Kip/Cip Family.

Foxg1 is highly expressed in proliferating cells of the neuroepithelium during neocortical development, while it declines in cells which had just left the mitotic cycle. *Foxg1* contributes to the development of telencephalon by maintaining telencephalic progenitor status and ensureing that such progenitors maintain appropriate cell cycle kinetics. In particular, *Foxg1* overexpression in neural stem cells induces the expansion of their compartment, perhaps by increasing NSCs self-renewal and survival [77]. As mentioned in the previous paragraph, Foxg1-/- mice show a reduced hemispheres size and a severely impaired ventral telencephalic development. That originates from reduced proliferation and increased differentiation [71,78,79].

It has been shown that *Foxg1* pro-proliferative activity largely depends on its capability to bind and inhibit the FoxO-Smad transcriptional complex, and in thus to obstruct p21 (Cip1) induction by Tgfb.

In this way, p21 cannot mediate the cell cycle arrest at G1 phase [80,81]. Furthermore, Foxg1 acts together with Polycomb factor Bmi-1, which upregulates *Foxg1* itself and repress cell cycle inhibitors p16, p19 and p21 [82].

Foxg1 in differentiation and migration of pyramidal neuron

Pyramidal neurons are born within the proliferative layers of the cerebral cortex [6], and during development they migrate to reach their final position. This occurs thanks to both radial and tangential migration. In the former case, radial glial fibers act as scaffold for their radial migration to the cortical plate; in the latter pyramidal neurons disperse tangentially, just like interneurons from ganglionic eminence [31].

When pyramidal neuron precursors lie within the intermediate zone, they transiently acquire a multipolar morphology, then they detach from the radial glia and initiate axonal outgrowth, before entering the cortical plate[28,83]. During these migratory phases, Foxg1 is expressed in a dynamic fashion. At the beginning of the multipolar phase it is transiently down-regulated in nascent pyramidal neuron precursors, allowing NeuroD1 and Unc5d expression, critical for the transition to the late multipolar phase. Failure in this down-regulation stalls pyramidal neuron precursors within the lower intermediate zone, delaying their entry in to the cortical plate and resulting in a switch in their laminar identity. Later, Foxg1 is specifically upregulated in order to induce the cells' exit from the multipolar phase and ingress into the cortical plate. Failure in Foxg1 upregulation in this phase leads to regression to the early multipolar phase and permanent loss of these cells. Thus, timing and duration of multipolar phase is finely regulated by Foxg1 dynamic expression, underlining the importance of the proper dosage of this gene [84].

Foxg1 is also fundamental for the correct lamination process of cortical progenitor cells. Neocortico-genesis needs the early specification of Cajal-Retzius pioneer neurons, then the following differentiation of deep layer neurons (DL) first and upper layer neurons (UL) after.

First, Foxg1 and Lhx2 instruct the cessation of the Cajal-Retzius cells' production, thus inducing progenitors to give rise to deep layer neurons [74,85]. As stated before, Foxg1 is induced by Fgf8 expressed in the anterior neural ridge[66] and subsequently expands caudally. Therefore, the onset of Foxg1 expression represses several transcription factors in an opposing rostral-to-caudal

gradient and regulates the transition from CR cell to DL neuron identity in a spatio-temporal dependent manner [85]. Moreover, Foxg1 is responsible for Tbr1 repression, which precedes the onset of Ctip2 and Fezf2, which mostly regulate deep layer specification. This suggest that Tbr1 repression by Foxg1 regulate the correct sequence of deep layer and upper layer neurons generation, by establishing the initial bias to deep layer identity [86]. Last but not least, high Foxg1 levels available in subgranular layers inhibit CouptfI transcripton, so resulting in further promotion of layer V differentiation programs, at expenses of layer IV ones [87].

Intriguingly, Foxg1 is present in both the nucleus and the cytoplasm: it is mainly confined in the nucleus in areas of active neurogenesis, while it is translocated to the cytoplasm in early neuronal differentiation areas [81]. Recently, a Foxg1 fraction localized in mitochondria has been illustrated, suggesting possible mechanisms for mitochondria in neuronal differentiation [88]. High Foxg1 levels detectable in post-mitotic glutamatergic neurons have been suggested to be crucial for their proper differentiation and function. As expected, *Foxg1* was recently described to promote elongation and arborization of neocortical pyramidal dendrites, via dedicated molecular cascades including *Hes1* and pCreb1 [89].

Foxg1 in astrogenesis control

It was shown that *Foxg1* over-expression in neural stem cells (NSCs) enlarged this compartment and reduced their astroglial output [77]. Results of this study led to hypothesize that this phenotype might stem from defective commitment of neural stem cells to glial fates. More recently, we demonstrated that this prediction was correct. We found that Foxg1 inhibits the transition from neural stem cell to committed astroblast, in mice as in humans, by means of a variety of concurrent molecular mechanisms. In this way, declining Foxg1 levels in aging neocortical stem cells allow to properly tune the onset of the astrogenic wave that fisiologically follows neuronogenesis, in late gestation embryos and neonate mice[90]. Intriguingly, these findings echo the old reports that two Drosophila *Foxg1* orthologs, *Sloppy paired-1* and -2 (*Slp1* and *Slp2*), promote neurogenesis at the expenses of gliogenesis [91] and Foxg1 can rescue the hypogliogenic *Slp1&2*-null phenotype [92].

FOXG1 and neurological disorders

FOXG1 syndrome is a condition characterized by impaired development and structural brain abnormalities. Affected infants are small at birth and show microcephaly by early childhood. The condition is associated with a particular pattern of brain malformations that includes a thin or underdeveloped corpus callosum, causing impaired connection between the right and left halves of the brain, reduced gyri on the surface of the brain, and a smaller amount of white matter [93].

As its name suggests, FOXG1 syndrome is caused by changes affecting FOXG1 gene. In some cases the mutation interests the gene itself, in others it also involves genetic material from a region of the long (q) arm of chromosome 14 that includes the FOXG1 gene. All of these genetic mutations lead to the production of a structurally abnormal Foxg1 protein and/or an altered dosage of it, resulting in an extremely complex spectrum of physical and neurological symptoms [93,94].

In particular, *FOXG1* results to be a highly dosage-sensitive gene: its shortage, indeed, disrupts normal brain development starting before birth. Deletions within 14q12 and inactivating mutations of FOXG1 are associated with Rett and Rett-like syndrome. Patients affected by this disorder show hypotonia, irritability, severe developmental delay, autism and microcephaly. In these individuals epilepsy, when present, does not start during infancy [95].

On the other hand, even a small increase in the dosage of *FOXG1* leads to neurological disorders. Patients with duplication of chromosome 14q12 showed infantile spasm and developmental delay of variable severity. Fifteen patient with 14dup. including *FOXG1* have been reported and nine of them presented epilepsy with a mean age at onset 4.9 months [96–98]. Expanding the phenotypic spectrum of *FOXG1*-related disorders, several authors showed that 14q12 duplications including *FOXG1* might be responsible of a subset of West Syndrome cases [95,99], a well-known severe epilepsy disorder composed of the triad of infantile spasms, an interictal electroencephalogram (EEG) pattern termed hypsarrhythmia, and mental retardation [100].

2. Aim

Aim of my study was to investigate the impact of Foxg1 in the regulation of neocortical neuron activity/excitability.

In order to cast light on the neurological aberrancies associated to FOXG1 copy number variations, I modulated its gene expression in primary neocortical neuronal cultures.

Molecular and functional analysis were performed to profile the consequences of Foxg1 abnormal gene dosage in these neurons and in the resulting network, as well as the underlying molecular mechanisms.

3. Materials and methods

Mouse handling

Animal handling and subsequent procedures were in accordance with European and Italian laws (European Parliament and Council Directive of 22 September 2010 [2010/63/EU]; Italian Government Decree of 04 March 2014, no. 26). Experimental protocols were approved by SISSA OpBA (Institutional SISSA Committee for Animal Care) and authorized by the Italian Ministery of Health (Auth. No. 1231/2015-PR of 25 November 2015).

Cortico-cerebral mixed cultures

Cortical tissue from E16.5 mice was chopped to small pieces for 5 minutes, in the smallest volume of ice-cold 1X PBS - 0,6% glucose - 0,1% DNaseI solution. The minced tissue was then resuspended and digested in 0.25 mg/ml trypsin- 4 mg/ml DNAseI for 5 minutes at 37°C. Digestion was stopped by adding ≥1.5 volumes of DMEM / F12 /10% FBS. Cortices were spinned down and transferred to differentiative medium [Neurobasal-A, 1X Glutamax (Gibco), 1X B27 supplement (Invitrogen), L-glutamate 25 µM, 25 µM β-Mercaptoethanol, 2% FBS,), 1X Pen/Strept (Gibco), 10 pg/ml fungizone (Gibco)]. Where required, 10 µM Cytosine β-D-arabinofuranoside "AraC" (Sigma) was acutely added to the medium. The suspension was pipetted 5-8 times with a P1000 gilson pipette and undissociated tissue was left to sediment for 1-2 minutes. The supernatant was harvested and the living cells counted. 1.0x106 or 0.5 x106 cells were plated on poly-L-Lysine coated 12-multiwell plates, in 600 µl of differentiative medium, in case of RTPCR/WB and immunoprofiling assays, respectively. Where indicated, lentiviral mixes were added to the cultures the day after plating (DIV1). Tet-regulated genes were activated by doxycyclin administration at DIV2.

Calcium Imaging

In the experimental groups of Foxg1-LOF and sister-control cultures, cells were incubated in 4 µM Fluo4-AM (Life Technologies, pre-dissolved in anhydrous DMSO (Sigma-Aldrich) at 4mM) and 0.01% Pluronic F-127 (Life Technologies; predissolved as 20% solution in DMSO), in Ringer's solution (145

mM NaCl, 3 mM KCl, 1.5 mM CaCl2, 1 mM MgCl2, 10 mM glucose and 10 mM Hepes, pH 7.4) at 37 °C for 1 hour (Ulloa Severino et al., 2016).

After incubation and upon washout in Ringer's solution, the cultures were visualised by a Nikon Eclipse Ti-U inverted microscope equipped with a piezoelectric table (Nano-ZI Series 500 µm range, Mad City Labs), an HBO 103 W/2 mercury short arc lamp (Osram, Munich, Germany), a mirror unit (exciter filter BP 465-495 nm, dichroic 505 nm, emission filter BP 515-555) and an Electron Multiplier CCD Camera C9100-13 (Hamamatsu Photonics, Japan). The experiments were performed at RT, and images were acquired using the NIS Element software (Nikon, Japan) with an S-Fluor 20X objective (0.75 NA) at a sampling rate of 5 Hz with a spatial resolution of 256 × 256 pixels for 10-15 min. The initial video was processed with the ImageJ (U. S. National Institutes of Health, Bethesda, MA) software. The image sequences were then analysed using a custom program design in MatLab. Appropriate regions of interest (ROIs) around the cells bodies were then selected.

For the experimental groups of Foxg1-GOF (generalized, astroglial and neuronal) and sister-control cultures, cells were incubated in 4 µM Oregon Green 488 BAPTA-1 AM (Invitrogen) in differentiative medium (see "Cortico-cerebral neuronal and mixed cultures") for 40 min (37 °C; 5 % CO2) [101,102]. The samples were then placed in a recording chamber mounted on an inverted microscope (Nikon Eclipse Ti-U) where they were continuously perfused at RT by a recording solution of the following composition (mM): 150 NaCl, 4 KCl, 1 MgCl2, 2 CaCl2, 10 HEPES, 10 glucose (pH adjusted to 7.4 with NaOH). Cultures were visualized with a 20 × objective (0.45 NA) and recordings were performed from visual fields (680 × 680 µm2, binning 4). Neurons positively stained by Ca2+ dye Oregon green 488 BAPTA-1 were simultaneously visualized within the sampled area and on average 30 ± 10 fluorescent cells were measured in each field.

Ca2+-dye was excited at 488 nm with a mercury lamp; excitation light was separated from the light emitted from the sample using a 395 nm dichroic mirror and ND filter (1/8). Images were continuously acquired (exposure time 150 ms) using an ORCA-Flash4.0 V2 sCMOS camera (Hamamatsu). The imaging system was controlled by an integrating imaging software (HCImage Live). At the end of each experiment, Tetrodotoxin (TTX, 1 µM, a voltage-gated, fast Na+ channel blocker; Latoxan) was applied to confirm the neuronal nature of the recorded signals. Recorded images were analysed off-line with Fiji (selecting ROIs around cell bodies), Clampfit software (pClamp suite, 10.2 version; Molecular Devices LLC, US) and Igor Pro Software (6.32 A version; WaveMetrics, Lake Oswego, Oregon, USA).

Intracellular Ca2+ transients were expressed as fractional amplitude increase (ΔF/F0, where F0 is the baseline fluorescence level and ΔF is the rise over baseline); we determine the onset time of neuronal activation by detecting those events in the fluorescence signal that exceed at least five times the standard deviation of the noise. Inter-event interval (IEI) values were calculated computing the difference between consecutive onset times, and IEI values obtained from each active cell in the field were pooled together. The correlation between the Ca2+ events among all active cells recorded from the same field was assessed by cross-correlation analysis using Igor Pro Software. The value of cross correlation function (CCF) was used to measure the strength of the correlation between cells, i.e. the relative probability that the peaks of calcium transients took place at the same time in all the cells.

All data are presented as mean ± standard error (SEM) of the mean. Statistical significance of differences in percentage of spontaneous active cells, cumulative IEI distribution, and CCF were evaluated with Chi-squared, Kolmogorov-Smirnov, and Mann-Whitney tests (Statistica 6.0—StatSoft, Italy), respectively. Differences between two data sets were considered statistically significant when $p < 0.05$.

Immunofluorescence

Immunofluorescence staining was performed according to standard methods. Briefly, neural cultures were fixed by 4% PFA for 20 min at 4 °C and washed 3 times in 1× PBS. Samples were subsequently treated with blocking mix (1X PBS; 10% FBS; 1mg/ml BSA; 0.1% Triton X100) for at least 1 hour at RT. After that, incubation with primary antibody was performed in blocking mix, overnight at 4°C. The day after, samples were washed in 1X PBS-0.1% Triton X-100 and then incubated with a secondary antibody in blocking mix, for 2 hours at RT. Samples were finally washed in 1X PBS, subsequently counterstained with DAPI (4', 6'-diamidino-2- phenylindole) and mounted in Vectashield Mounting Medium (Vector).

The following primary antibodies were used: anti-GFP, chicken polyclonal (Abcam ab13970, 1:400); anti-Foxg1, rabbit polyclonal (gift from G.Corte, 1:200); anti-Tubβ3, mouse monoclonal, (clone Tuj1, Covance MMS-435P, 1:1000); anti-NeuN, mouse monoclonal (clone A60, Millipore MAB 377, 1:80); anti-GFAP, rabbit polyclonal (DAKO Z0334, 1:500); anti- S100β, rabbit polyclonal (DAKO Z0311,

1:300); Secondary antibodies were conjugates of Alexa Fluor 488, and Alexa Fluor 594 (Invitrogen, 1:600).

Photography and image processing

Immunoprofiled cell preparations were photographed on a Nikon TI-E microscope, equipped with 20X or 40X objectives and a Hamamatsu C4742-95 camera. All images were processed using ImageJ software.

RNA-Seq profiling

Sample preparation. Neural cultures were set up from neocortices of wt, CD1 strain, E16.5 embryos, as described above. At DIV1 they were alternatively infected by lentiviral sets "LV_pPgk1-rtTA2S-M2 & LV_TREt-Foxg1" (Foxg1-GOF samples) and "LV_pPgk1-rtTA2S-M2 & LV_TREt-Plap" (control samples), each virus at moi=8, and four biological replicates were generated for each LV combination. On the same day AraC was added to the medium to a final 10 ?M concentration. At DIV3 the transgenes were activated by adding 2 ?g/ml doxycycline to medium. Five days later, at DIV8, cells were lysed and RNA extracted by TrizolTM (ThermoFisher).

Library preparation and sequencing. Upon quality control (RIN>7), the 4+4 RNA samples were processed by Stranded mRNA-Seq Illumina TrueSeq kit. Then, >20M reads per sample (paired-ends, 75bp) were collected, by NextSeq500 technology.

Data pre-processing. After a primary check of raw sequencing data by FastQC, low quality read portions were removed with BBDuk (minimum read length set to 35 bp and minimum base quality score to 25). Reads passing this filter (>99% of primary ones) were aligned with STAR aligner 2.5.0c against Mus musculus reference genome (Ensembl GRCm38). Here, 98% of the reads could be mapped, about 91% uniquely, 7% with multiple mappings. Next, FeatureCounts 1.6 and Mus musculus GRCm38.91 annotation were used to calculate gene expression values, first as raw read counts and then as normalized FPKM values.

Data analysis. It was performed in R with HTSFilter and edgeR packages. First, not expressed genes and those showing too much variability were removed with HTSFilter. Specifically, the algorithm

calculated the Global Jaccard index (GJi) of similarity between the samples, as a function of different minimum “Trimmed Means of M-values” (TMM)-normalized read counts (s). GJi peaked when s equalled 86.228 and, consequently, this value was used as a threshold. All the loci with TMM normalized read counts below it were removed. In this way, about 11,500 out of 53,000 genes passed the HTSFilter. Next, upon control of replicates quality, genes differentially expressed between Foxg1-GOF and control groups were scored. For each of them the "false discovery rate" (FDR, according to Benjamini-Hochberg) and the "fold change" (FC) were calculated. Genes were considered significantly differentially expressed if FDR≤0.05 and $p<0.05$. 7,582 differential expressed (DE) genes were detected. For 3,434 of them, $-1 \leq \log2FC \geq 1$. Steps 2-4 were entrusted to a commercial operator (Sequentia, Barcelona, Spain).

Quantitative RT-PCR

In each experimental session, aliquots of 1x106 cells were processed for RNA extraction by TrizolTM Reagent (ThermoFisher) according to manufacturer’s instructions. RNA preparations were treated by TURBOTM DNase (2U/µl)(AmbionTM) 1 hour at 37 °C. At least 0.75 µg of genomic DNA-free total RNA from each sample was retro-transcribed by SuperScriptIIITM (Invitrogen) in the presence of random hexamers, according to manufacturer’s instructions. 1/100 of the resulting cDNA was used as substrate of any qPCR reaction. Limited to intronless amplicons, negative control amplifications were run on RT(-) RNA preparations. PCR reactions were performed by SsoAdvanced SYBR Green SupermixTM (Biorad), according to manufacturer’s instructions. Per each transcript under examination and each sample, cDNA was PCR-analyzed at least in technical triplicate and results averaged. When not otherwise specified, averages were further normalized against Gapdh. Experiments were performed at least in biological triplicates and analyzed by Student’s t test. The following oligonucleotides have been employed in this study:

ARC/F 5’ CCC TCA TCT GTC TGC CCT GG

ARC/R 5’ ACC CAA AGA GCC CTG GAC AC

BDNF4/F 5’ CTG CCT TGA TGT TTA CTT TGA CAA GTA GTG ACT G 3’

BDNF9/R 5’ GCC TTC ATG CAA CCG AAG TAT GAA ATA ACC ATA G 3’

CACNA2D2/F 5’ CGT ACC CAT CAG GAC CAA CC 3’

CACNA2D2/R 5’ CCT GGT CCC ACT GAT GGT TC 3’

Cebpb/F 5’ CAA CCT GGA GAC GCA GCA CAA GGT G 3'

Cebpb/R 5’ GGG CAG CTG CTT GAA CAA GTT CCG 3'

D2GFP/F 5’ TCA TGT CTG CTC GAA GCG GC 3’

D2GFP/R 5’ GCA CGC TGC CCA TGT CTT GT 3’

GAD1/F 5’ ACC AGT TGC TGG AAG GCA TGG AAG G 3’

GAD1/R 5’ AGA GCT GGT TGA AAA ATC GAG GGT GAC 3’

GAD2/F 5’ ATA ATT GGG AAT TGG CAG ACC AAC CGC 3’

GAD2/R 5’ CTG CTG CTA ATC CAA CCA TAT CCA ATC C 3’

Grik3/F 5’ GTC GCC CAT CGA CTC CGC TGA TG 3’

Grik3/R 5’ TCA GCT GTG AGC GTC CGC TGG AT 3’

Grik4/F 5’ CGA GCT TTG TCT ACC CGC TGT GTC A 3’

Grik4/R 5’ GTC AGC CAG GTC ATC CAC AGA CTC AA 3’

Grin2A/F 5’ CTC ACC CTG GAA GAG GCA GAT TGA C 3’

Grin2A/R 5’ AGC CAG CAT GTA GAA AAC TCC TGC CA 3’

Grin2c/F 5’ CTG GAT TTC GTC TCC TCT CAG ACC C 3’

Grin2c/R 5’ GTA TTC CTC CAG CAC CTT GAA CAG CAC 3’

mEgr1/F1 5' AAC CCT ATG AGC ACC TGA CCA CAG AGT C 3'

mEgr1/R1 5' CGT TTG GCT GGG ATA ACT CGT CTC CAC 3'

mEgr2/F1 5' AGG CCC CTT TGA CCA GAT GAA CGG AGT 3'

mEgr2/R1 5' GTT TCT AGG TGC AGA GAT GGG AGC GAA G 3'

mFos/F1N 5' CTG ACA GAT ACA CTC CAA GCG GAG ACA G 3'

mFos/R1N 5' ACA TCT CCT CTG GGA AGC CAA GGT CAT C 3'

mFoxg1.3'utr/F: 5' AGG AAG GTT GTT TAG TTG GCA ACA CTG C 3'

mFoxg1.3'utr/R: 5' GTG ACC TGT TAG TGA CCA CAT ACA TCG AA 3'

mFoxg1.5'utr/F: 5' TAG AAG CTG AAG AGG AGG TGG AGT GC 3'

mFoxg1.5'utr/R: 5' CAG ACC CAA ACA GTC CCG AAA TAA AGC 3'

mFoxg1.cds/F 5’ CGA CCC TGC CCT GTG AGT CTT TAA G 3’

mFoxg1.cds/R 5’ GGG TTG GAA GAA GAC CCC TGA TTT TGA TG 3’

mGapdh5/F 5’ ATC TTC TTG TGC AGT GCC AGC CTC GTC 3’

mGapdh5/R 5’ GAA CAT GTA GAC CAT GTA GTT GAG GTC AAT GAA GG 3’

mmuGabra1/F 5' AAA CCA GTA TGA CCT TCT TGG ACA AAC AGT TGA C3'

mmuGabra1/R 5' GTG GAA GTG AGT CGT CAT AAC CAC ATA TTC TC 3'

mSCN1a/FW 5' TGT GCC CAT TGC TGT GGG AGA GTC T 3'

mSCN1a/RV 5' TCT GAG GAG CTA CTG CTT TCG TTG AGT TT 3'

RFP/F 5’ AGA AAA CAC TCG GCT GGG AG 3’

RFP/R 5’ CCG GGC ATC TTG AGG TTC TT 3’

SCN11a/F 5’ AGC GCC TTG TTT TCT CGG TA 3’

SCN11a/R 5’ CCC ACG ATG ACC TTC AGA CC 3’

Western blot analysis

Western blot analysis was performed according to standard methods. Total cell lysates in CHAPS buffer were quantified by BCA protein assay kit (Fisher Scientific #10678484) and denatured at 95°C for 5 min, prior to loading. Thirty micrograms of proteins were loaded per each lane on a 10% acrylamide - 0.1% SDS gel. Foxg1 was detected by a primary rabbit anti-Foxg1 polyclonal antibody [77], used at 1:2000 dilution, and a secondary goat HRP-conjugated anti-rabbit polyclonal antibody (DAKO P044801), used at 1:2000 dilution. βACT was detected by a HRP-conjugated mouse monoclonal antibody (Sigma #A3854), used at 1:10,000 dilution. Foxg1 and βACT were sequentially revealed by an ECL kit (GE Healthcare #GERPN2109). Images were acquired by an Alliance LD2–77.WL apparatus (Uvitec, Cambridge) and analyzed by Uvitec NineAlliance software.

Statistical analysis

Generally, when not otherwise stated, experiments were performed at least in biological triplicate. Results were normalized against controls and their statistical significance was evaluated by the t-test (one-tail; unpaired).

Lentiviral production and titration

Third generation self-inactivating (SIN) lentiviral vectors (LTVs) were produced as previously described [103] with some modifications. Briefly,293T cells were co-lipofected (LipoD293TM, SigmaGen) with the transfer vector plasmid plus three auxiliary plasmids (pMD2 VSV.G; pMDLg/pRRE; pRSV-REV).The conditioned medium was collected after 24 and 48hs, filtered and ultra-centrifuged at 50000 RCF on a fixed angle rotor (JA 25.50 Beckmann Coulter) for 150 min at 4°C. Viral pellets were resuspended in PBS without BSA (Gibco). LTVs were generally titrated by Real Time quantitative PCR after infection of HEK293T cells, as previously reported (Sastry et al., 2002). One end-point fluorescence-titrated LTV was included in each PCR titration session and PCR-titers were converted into fluorescence-equivalent titers throughout the study.

Lentiviral plasmids construction

Basic DNA manipulations (extraction, purification, and ligation) as well as bacterial cultures and transformations, media and buffer preparations were performed according to standard methods. Restriction and modification enzymes were obtained from New England Bioloabs and Promega;DNA fragments were purified from agarose gel by the QIAquick Gel Extraction Kit(Qiagen); small and large scale plasmid preparations were done by DNA plasmid purification kit (Qiagen). Plasmids were grown in E.Coli, Xl1-blue or ElectroMAX™ Stbl4™ Competent Cells (Invitrogen).

4. Results

Hyperactivity of *Foxg1*-GOF neocortical cultures

To test the hypothesis that *Foxg1* overexpression increases neocortical activity, we generated *Foxg1*-LOF/GOF neocortical cultures by somatic lentiviral transgenesis and probed them by fluorescence calcium imaging. In these experiments, the expression of our gene was dampened by RNAi or, alternatively, upregulated by TetON/OFF transgenesis. RNAi was achieved by a shRNA transgene, driven by an ubiquitous U6 promoter. As for GOF manipulations, four different promoters, limiting *Foxg1* over-expression to specific compartments of the culture, were employed:

- Phosphoglycerate Kinase 1 (Pgk1) promoter, generalized expression
- Synapsin 1 (Syn) promoter, neuron-specific expression
- Glial Fibrillary Acidic Protein (GFAP) promoter, astrocyte-specific expression
- Ca2+/calmodulin-dependent kinase (CaMK) promoter, glutamatergic neuron-specific expression

The assays were generally run on mixed neuronal-astrocytic cultures originating from neocortex of E16.5 wild type mouse embryos. As for GOF assays, these cultures were engineered according to a TetON design, with two lentiviral vectors, harboring a variable "neural promoter-*rtTA.M2* transgene" and a "TREt-*Foxg1* transgene" (or its control), respectively. The platform was slightly different in the case of glutamatergic neuron-restricted *Foxg1* over-expression. These experiments were carried out by a TetOFF system, taking advantage of transgenic mice expressing the tTA under the control of the CaMKII promoter and transducing neural cultures originating from their neocortex with a lentiviral a "TREt-*Foxg1* transgene" (Fig. 6A).

In all cases, cultures were terminally treated by Ca^{2+}-sensitive fluorescent dies and fluorescence fluctuations were recorded and analyzed by dedicated software. Three indices, representative of culture activity, were calculated: (a) prevalence of spontaneously active neurons among total neurons; (b) cumulative distribution of inter-event intervals (IEIs, i.e. inter-calcium transients intervals); (c) neuronal activity cross-correlation factor (CCF).

We found that *Foxg1* knock-down reduced the prevalence of spontaneously active neurons (49% vs 83%, with $p<0.001$ and n=4,4), as well as their CCF (0.14±0.001vs 0.79±0.002, with $p<0.001$ and n=4,4) (Fig. 6B). Moreover, *Foxg1*-LOF cultures were characterised by transient high frequency bursts of activity interspersed by prolonged silent periods , resulting in a peculiar cumulative distribution of IEIs ($p < 0.01$). In a few words, knocking down *Foxg1* caused a complex alteration in network dynamics, characterized by unevenly distributed calcium transients, restricted to less numerous, hypo-synchronized neurons.

As expected, generalized *Foxg1* overexpression conversely increased the prevalence of spontaneously active neurons (94% vs 18%, with $p<0.01$, n=3,3) (Fig. 6C), as well as their CCF (0.90±0.04 vs 0.19±0.02, with n=3,1), while prevalently shortening their IEIs ($p<0.01$). That points to a strong functional impact of pan-neural *Foxg1* upregulation on synaptic networks.

Next, when *Foxg1* overexpression was limited to astrocytes, neither the prevalence of active neurons (29% vs 30%, with n=5, 4) nor their CCF (0.9±0.02 vs 0.8±0.02, with n=5,4) were affected (Fig. 6D). Instead, IEIs were significantly increased ($p<0.01$). This means that *neuronal Foxg1* upregulation is *necessary* to enhance network activity. It further suggests that *Foxg1*-GOF astrocytes may somehow dampen neuronal activity better than control astrocytes.

Restriction of *Foxg1* overexpression to the neuronal lineage increased the prevalence of active neurons (98% vs 31%, with $p<0.001$ and n=12, 12) (Fig. 6E), and their CCF (0.98±0.01 vs 0.40±0.01, with $p<0.001$ and n=12,12), while shifting cumulative distribution of IEIs significantly to the left ($p<0.001$). This means that neuronal *Foxg1* upregulation is not only necessary, but also *sufficient* to elicit a powerful stimulating effect on network activity.

Finally, when GOF was restricted to glutamatergic neurons, a higher percentage of spontaneously active neurons was again detected (94% of 231 GOF cells vs 67% of 235 control cells (Fig. 6F), their firing rate was also increased (see representative fluorescent traces in figure 6F, panel 2). CCF was however poorly affected (0.74 ± 0.14 vs 0.66 ± 0.13). This indicates that *interneuronal Foxg1*-overepression specifically promotes network synchronization.

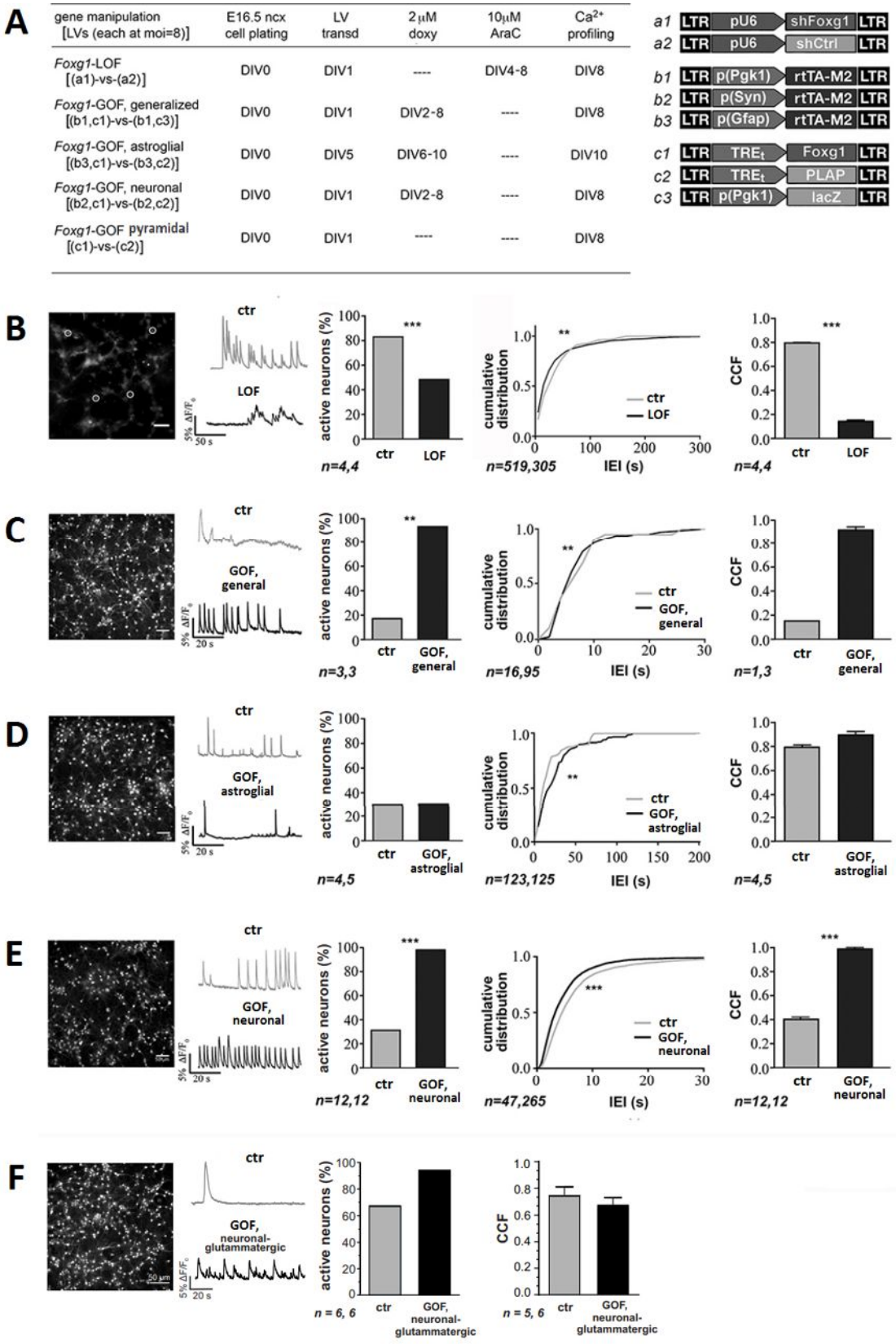

Figure 6. Evaluation of neocortical culture activity upon Foxg1 expression level modulation, by real time Ca2+

Interneuron depletion

Encouraged by the outcome of calcium imaging assay, we further wondered if a misregulation of the GABAergic-to-glutamatergic neuron ratio could occur in those cultures and contribute the observed phenotype. To address this question, we set up cultures of E16.5 neocortical precursors originating from *Gad1*$^{EGFP/+}$ donors [104], expressing EGFP in all GABAergic neurons. Cells were engineered as described for calcium imaging experiments (Fig. 7A), and the EGFP^{+}NeuN^{+}/NeuN^{+} cell ratio at DIV8 was evaluated. We found that generalized and neuron-restricted *Foxg1* overepression (driven by *Pgk1* and *Syn* promoters, respectively), decreased this ratio from 16.8±0.6% to 10.5±1.1% ($p<0.001$, n=4,4) as well as from 10.6±0.4% to 4.0±0.7% ($p<0.0001$, n=4,4), respectively (Fig. 7B, graphs 2, 4). Astrocyte- and pyramidal neuron-confined *Foxg1* overexpression were uneffective (Fig. 7B, graph 3, 5). Knock-down of endogenous *Foxg1* reduced this ratio only to a very limited extent, from 13.8±0.4% to 12.7±0.4% ($p<0.04$, n=4,4) (Fig. 7B, graph 1). In other words, a pronounced interneuron depletion took place upon neuronal *Foxg1* upregulation, likely contributing to network hyperactivity evoked by manipulation. However, this depletion did not occur when interneurons were not genetically manipulated, suggesting the occurrence of cell-autonomous cytotoxic phenomena, triggered within these cells by *Foxg1* over-dosage.

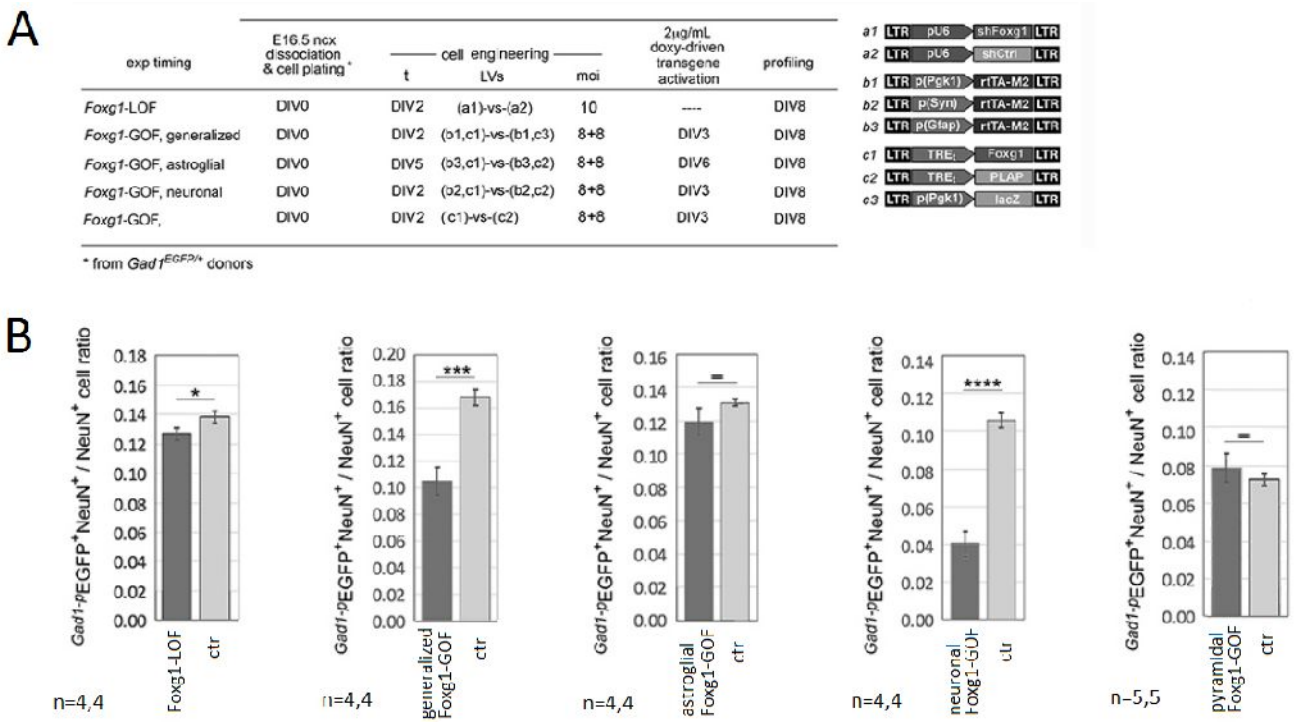

Figure 7. Interneuron quantification in Foxg1-GOF neocortical cultures.

Misregulation of *Foxg1*-GOF neocortical neuron transcriptome.

To cast light on molecular mechanisms underlying over activity of *Foxg1*-GOF neurons, we profiled the transcriptome of neuronal cultures originating from E16.5 neocortical precursors, transduced by a broadly expressed *Foxg1* transgene and allowed to age up to DIV8 in the presence of AraC. Four *Foxg1*-GOF and four control cultures were profiled. >20M paired reads/sample were collected and aligned against the reference genome, raw read counts were normalized as FPKM values, and results were finally filtered according to standard procedures. 11,500 out of 53,000 genes passed filtering. Among them, 7582 resulted to be differentially expressed in *Foxg1*-GOF vs control cultures (with $p<0.05$ and FDR<0.05). 3876 were upregulated (1816 of them >2-folds) and 3706 downregulated (1631 of them >2-folds). As positive controls, total *Foxg1*-mRNA was increased by 4.4-folds, *Arc* and *Hes1*, expected to robustly arise upon *Foxg1* overexpression [89], were upregulated as well, by 6.6-folds ($p<5.31*10-54$, FDR<2.53*10-52) and 34.9-folds ($p<1.12*10-136$, FDR<2.93*10-134), respectively, *Emx2* and *Tbr1*, normally dampened by *Foxg1* [86,105], were downregulated by -50.1% ($p<1.26*10-03$, FDR<3.57*10-03) and -14.5% ($p<8.31*10-03$, FDR<1.93*10-02), respectively.

To get hints about molecular mechanisms underlying abnormal activity of *Foxg1*-GOF neurons, we focused our attention on specific sets of differentially expressed genes, linked to intracellular signal integration and synaptic transmission. Among them, genes encoding for:

(1) plasmamembrane, voltage-dependent Na^+, K^+ and Ca^{2+} channels, incuding those belonging to Scn, Kcn and Cacn families [106–109], as well as pumps and channels mediating Ca^{2+} fluxes among cytoplasm, ER, mitochondria and extracellular spaces, i.e. PMCAs, NCXs, NCKXs, SERCAs, MCU-, SOCE-, CICR- and IICR-effectors [110,111];

(2) glutamatergic and GABAergic receptors (Grm, Gria, Grik, Grin, Gabr) [112–114];

(3) neuromodulator receptors (Chrm, Chrn, Adr, Htr, Drd, P2rx, P2ry)[115];

(4) selected structural components of synapses [116]. Results were highly articulated and included a large subset of expression level variations likely contributing to enhanced neuronal activity and synchronization.

We found a widespread upregulation of *Scn* genes. *Scn1a*, mainly restricted to PV^+ interneurons and required for their inhibitory activity [117], was conversely decreased by about 4-folds. Quantification of Kcn genes did not show any simple shared trend. *Kcc2*, promoting the transition from GABA-driven depolarization to hyperpolarization [118,119], was upregulated >3-folds. Members of *Cacna1*, *Cacnb* and *Cacng* subfamilies were prevalently increased and the *Cacna2d2/Cacna2d1* ratio was specifically upregulated by about 28-folds, all pointing to a possible increase of Cacn-dependent Ca^{2+} currents [120]. A complex expression pattern was also displayed by other genesets mastering Ca^{2+} exchanges among cytoplasm and other cell compartments. Implicated in Ca^{2+} extrusion to cell exterior, PMCA-encoding *Atp2b2-4* and NCX-encoding *Slc8a1-3* were upregulated, NCKX-encoding *Slc24a2,4* down-regulated. SOCE effector-encoding genes *Stim1* and *Orai2*, promoting Ca^{2+} influx from cell exterior, were upregulated. Involved in release of ER Ca^{2+}, CICR- and IICR machinery genes Ryr1,2 and Itpr1,3, were down- and up-regulated, respectively. SERCA-encoding *Atp2a2*, implicated in ER Ca2+ uptake, was downregulated. Finally, three repressors of the MCU machinery, mediating mitochondial Ca^{2+} uptake, *Mcub*, *Micu2* and *Micu3*, were downregulated, and its stimulator Slc25a23 was upregulated, altogether prefiguring an increased activity of this machinery.

Next, genes encoding for ionotropic glutamatergic receptors showed a pattern definitively consistent with increased neocortical activity. *Grik1*, restricted to interneurons [121], was downregulated, *Grik3*, active in pyramids and encoding for the principal GluK3 subunit [122], was upregulated, *Grik4* and *Grik5*, both essential for the normal ionotropic function [123], were increased as well. As for *Gria* family, both *Gria2*, decreasing Ca2+ permeability of AMPA receptors [124], and *Gria4*, needed to prevent epileptic seizures [125], were downregulated. Finally, concerning Grin genes, in addition to *Grin1* decline, Grin2c/Grin2a and Grin2d/Grin2a ratios were dramatically upregulated, pointing to likely prolonged opening times of NMDA receptors [126]. Grin3, normally limiting Ca2+ permeability of these receptors [127], was downregulated. Moreover, a collapse of key genes implicated in GABA-ergic conduction and GABA-mediated homeostasis, *Gad1, Gad2, Gabra1, Bdnf* [128], was also detected.

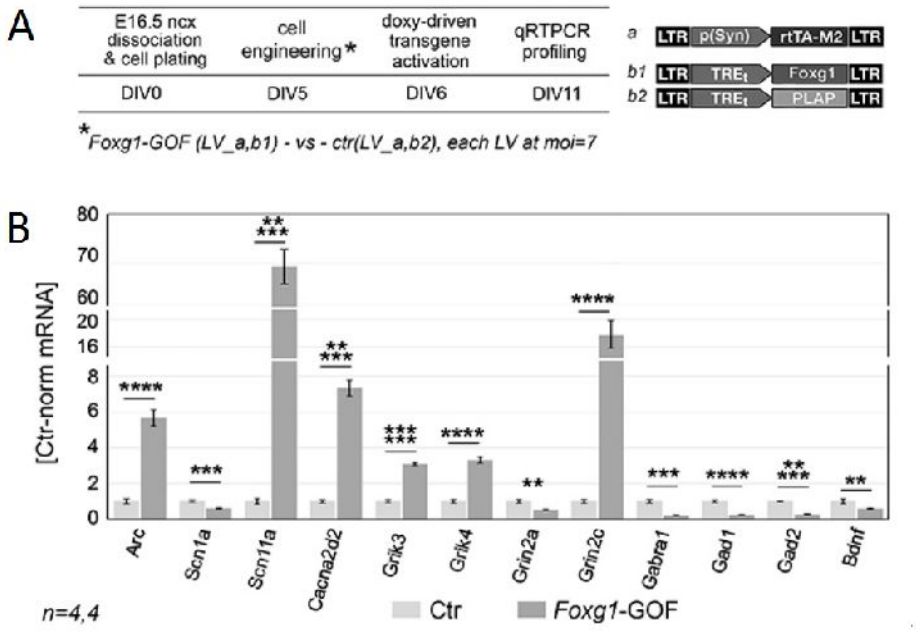

*Figure 8. qRTPCR profiling of neocortical cultures overexpressing Foxg1 in their neuronal compartment. (A) Protocol, (B) results. Data evaluated by t-test (unpaired, one-tailed). ** p<10-2, *** p<10-3, **** p<10-4, ***** p<10-5, ****** p<10-6. n = number of biological replicates, i.e. indepen-dently transduced cell samples.*

Dynamics of neuromodulator receptor genes [115] was very complex. It included alterations with a potential pro-excitatory (*Chrnb4*, *Adra1b*, *Htr3a*, *Htr6* and *P2rx4* upregulation, as well as Grm2 and Grm8 decline) or pro-inhibitory outcome (*Adra1a* and *P2rx2* downregulation as well as Grm4 and

Drd2 upregulation). Similar considerations apply to modulation of structural synaptic genes, some upregulated (e.g., *Homer2*, *Nrxn2,3* and *Shank1*,2), some decreased (e.g. *Homer1, Nlgn1*).

To strengthen these results, we evaluated mRNA levels of a subset of differentially expressed genes, in sister preparations of Foxg1-GOF cultures employed for Ca2+ imaging assays, by qRTPCR. To note, here we restricted Foxg1 overexpression to neurons, under the control of pSyn promoter. Moreover, we omitted AraC, so allowing neurons to mature in more biologically plausible conditions, i.e. in the presence of a large astrocyte complement. Interestingly, qRTPCR analysis of these samples reproduced the variation pattern previously detected in RNASeq assays (Scn11a, Grik3, Grik4 and Grin2c upregulated, Scn1a, Grin2a, Gabra1, Gad1, Gad2 and Bdnf downregulated, Fig. 8B), corroborating the scenario emerging from these assays. The complete dataset is available at https://zenodo.org/record/2849657.

Activity-dependent Foxg1 upregulation in neocortical neurons and its molecular control

A reciprocal positive feedback between two network nodes may robustly enhance the output of either node, following an even moderate increase of (a) exogenous inputs feeding them or (b) internode connection weights. In this way, an even subtle alteration of these parameters may result in dramatic changes of the network state. In this respect, we wondered if, able to promote neuronal activity, *Foxg1* would be in turn stimulated by such activity.

To address this issue, we transferred DIV6.5 neural cultures originating from E16.5 neocortical tissue under 25 mM extracellular K^+, namely a robust depolarizing treatment [129], and monitored temporal progression of *Foxg1*-mRNA and -protein (Fig. 9). Both gene products underwent a substantial, transient upregulation. The former arose as early as at 1 hour, peaked up at 3 hours (about 2.75-folds) and later declined, getting back to baseline values by 18-24 hours (Fig. 9A). The latter showed an appreciable increase already at 6 hours, peaked up at around 12 hours (about 1.75-folds) and later declined, rebounding to halved levels at about 24 hours (Fig. 9B).

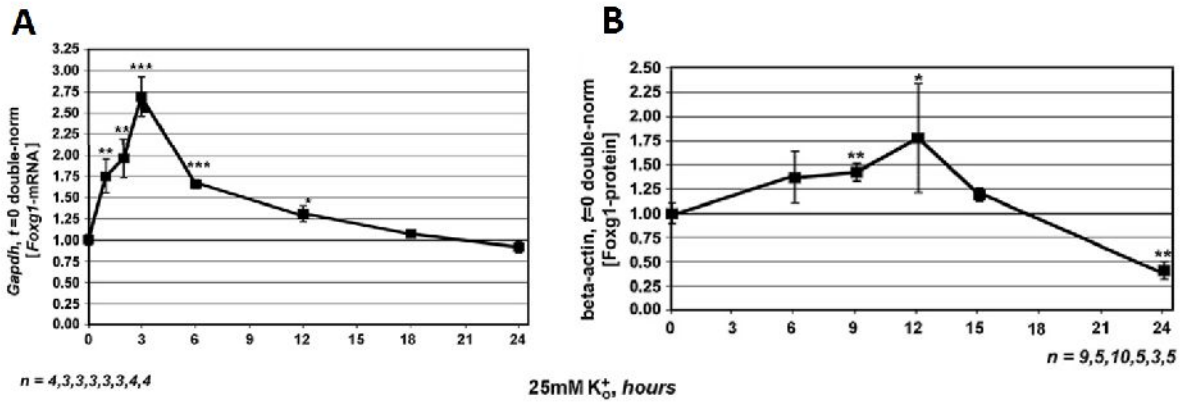

Figure 9. Activity-dependent modulation of neocortical Foxg1 expression levels in dissociated DIV7 cultures originating from E16.5 neocortical tissue. (A) qRTPCR quantification of Foxg1-mRNA in cultures stimulated by 25 mM K+ for 0-24 hours; (B) WB quantification of Foxg1-protein in cultures stimulated by 25 mM K+ for 1-24 hours. Data kindy provided by Moira Pinzan and Osvaldo Artimagnella.

Looking for mechanisms underlying activity-dependent Foxg1 regulation, we noticed that the Foxg1 transcription unit and its surroundings are rich in binding sites for immediate early gene-encoded transcription factors (ieg-TFs), validated by Chromatin-Immuno-Precipitation (ChIP) in non neural cell lines (as reported in UCSC Genome Database) or predicted *in silico* by Jaspar software[130] (Fig. 10).

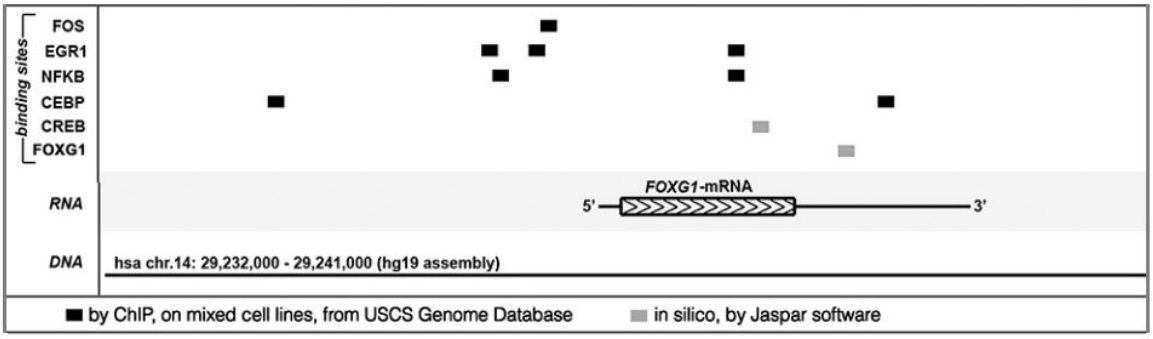

Figure 10. Selecting putative mediators of Foxg1 response to high K+. (A) Localization of immediate early gene factors and Foxg1-binding sites within the Foxg1 locus, as detected by ChIP on selected cell lines (UCSC), or predicted by Jaspar software.

Therefore, we hypothesized that these TFs, including pCreb1, nuclear-RelA^{p65}, Fos, Egr1, Egr2 and Cebpb, might be instrumental in such regulation. Functional knock-out of these ieg-TFs was carried out in our lab in order to test this prediction. All six ieg-TFs under analysis resulted instrumental for Foxg1 transcription, since in their absence Foxg1-mRNA resulted down-regulated by about 15-40% (unpublished data). Next, we wondered whether temporal progression of these TFs would be etiologically compatible with *Foxg1*-mRNA fluctuations, in primary neocortical cultures challenged by high potassium. Previous data about the behavior of *Fos-, Egr1-, Egr2-* and *Cebpb*-mRNAs show how they peaked up at 1 hour and then declined (unpublished data), consistently with an involvement of them in *Foxg1*-mRNA peaking at 3 hrs. pCreb1 and nuclear-RelA^{p65}, normally tuned by fast post-translational mechanisms [117,131,132], were quantified by immunofluorescence: they peaked up as early as at 20 min and remained above the baseline at least up to 90 min (Fig. 11).

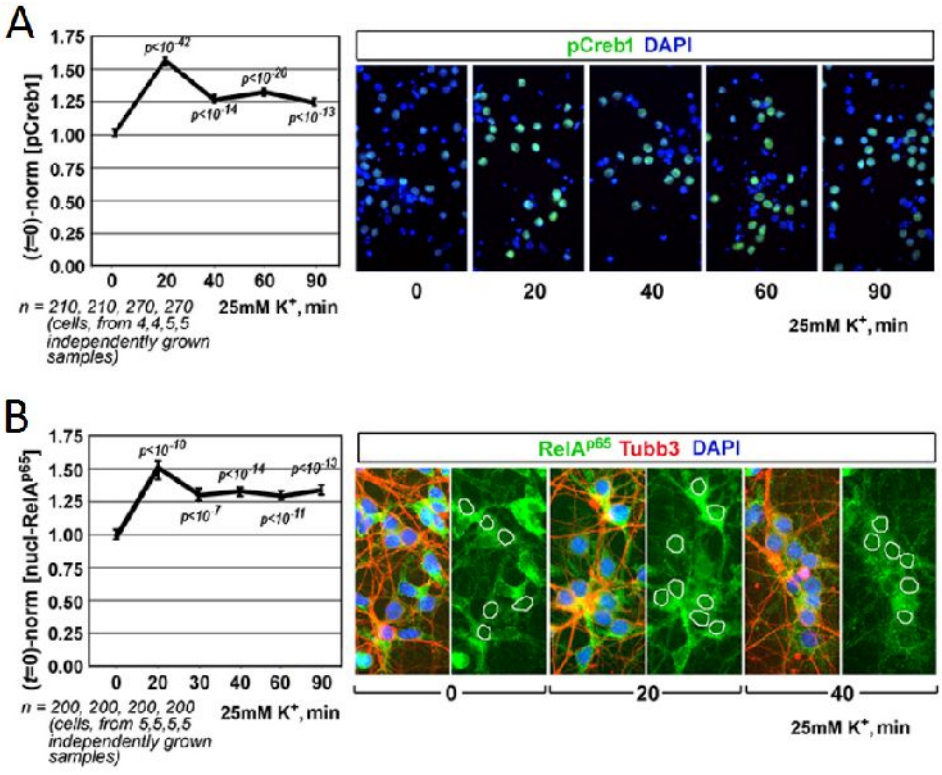

Figure 11. Fluctuations of pCreb1 (A) and nuclear RelA^{p65} evoked by timed exposure of dissociated DIV7 cultures originating from E16.5 neocortex to 25 mM K$^+$. Quantification by quantitative immune fluorescence.

We further investigated the potential impact of these two TFs, monitoring their activity by means of dedicated molecular reporters. As expected, the *d2EGFP*-mRNA products of the pCreb1- and NFkB-activity reporters cAMP.RE3-p(min)-d2EGFP and NFkB.BS4-p(min)-d2EGFP, pre-delivered to neural cells by lentiviral transgenesis) displayed also an early-onset, transient upregulation (Fig. 12). In synthesis, activity-dependent elevation of *all six effectors* preceded *Foxg1*-mRNA arousal. As such, all the former ones could be instrumental in achieving the latter.

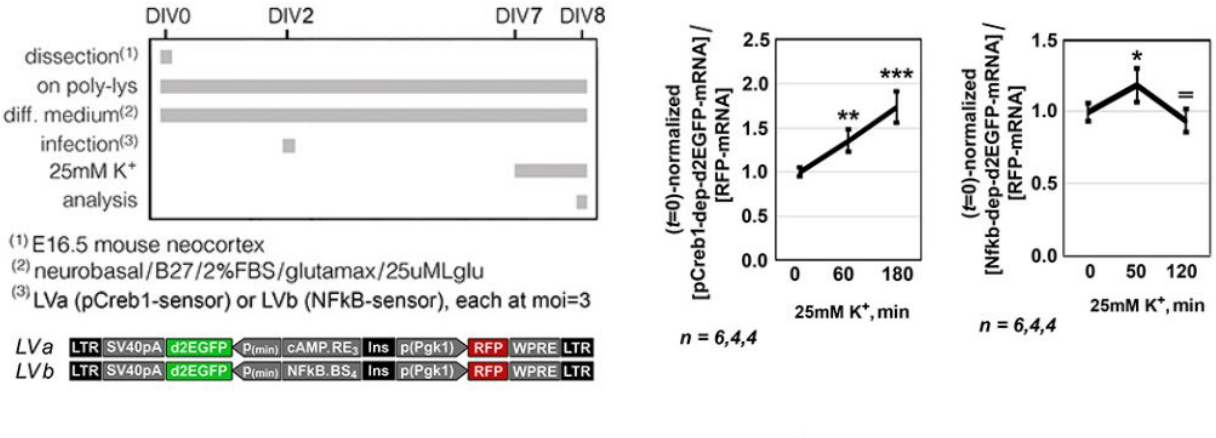

Figure 12. qRTPCR evaluation of pCreb1 and RelA^{p65} pro-transcriptional activities in dissociated DIV7 cultures originating from E16.5 neocortex, upon exposure to 25 mM K$^+$.

Hyperactivation of iegs in K+-stimulated, Foxg1-GOF neocortical cultures

We have shown that a reciprocal positive feedback may take place between *Foxg1* overexpression and neocortical activity. This feedback might robustly influence neocortical activity regime, strengthening the electro-clinical phenotype of *Foxg1*-GOF mice and exacerbating EEG abnormalities of human patients with a supranumerary *FOXG1* allele. To get an insight into these phenomena, we investigated the impact of increased *Foxg1* expression on K$^+$-stimulated neocortical cultures. To this aim, *Foxg1* was upregulated by gentle RNAa (Fig. 13A), eliciting a 1.5x - 2.0x expression gain, presumably close to that caused by FOXG1 duplications, and complying with activity-dependent gene tuning [133]. Then, neural cultures were profiled for activity and expression of selected iegs (Fig. 13B, C), as proxies of ongoing neuronal activity[131] and - meanwhile - promoters of it [134–140]. Interestingly, following K$^+$ stimulation, the d2EGFP-mRNA product of the pCreb1-activity

reporter was rapidly upregulated in Foxg1-GOF samples compared to controls (ctrt=0-normalized levels at 1 hour were 1.74±0.11 vs 1.36±0.13, respectively, with p<0.032) (Fig. 13B). The corresponding NFkB-activity reporter, upregulated at 50 min in both Foxg1-GOF samples and controls (1.15±0.03 and 1.19±0.12, respectively, with p=0.296), retained its overexpression at 2 hours in the former, while declining in the latter (1.22±0.14 vs 0.94±0.08, with p<0.003) (Fig.13B). Cebpb-mRNA was conversely upregulated in Foxg1-GOF samples for at least 6 hours after high K^+ exposure (for example, ctrt=0-normalized levels at 2 hours were 4.96±0.39 and 3.64±0.24, in GOF and ctr samples, respectively, with p<0.016) (Fig. 13C).

Previous experiments in our lab pointed out a consistent scenario regarding the quantitation of endogenous Fos, Egr1. Peaking at 1 hour in Foxg1-GOF samples like in controls, both Fos- and Egr1-mRNAs showed a delayed rebound towards baseline in Foxg1-GOF samples compared to controls (Tigani, Pinzan et al., submitted). Altogether, these results suggest that, upon hyper-stimulation, neocortical *Foxg1*-GOF networks may display a more prolonged and sustained activity compared to their control counterparts.

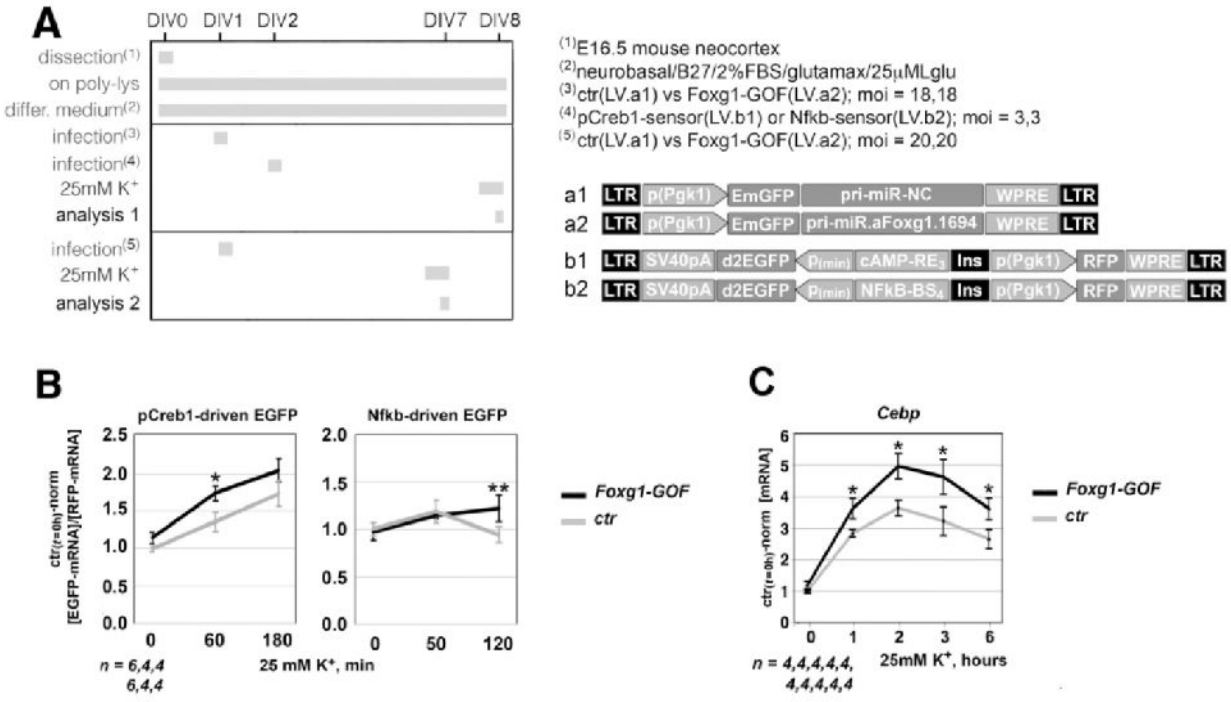

Figure 13. Foxg1-driven modulation of ieg response to high K+. (A) protocol; (B) qRTPCR evaluation of pCreb1 and NFkb transcriptional activities; (C) qRTPCR evaluation of Cebpb mRNA levels. .

5. Discussion

To investigate on the impact of Foxg1 on neocortical neuronal activity we generated *Foxg1*-GOF neocortical cultures by somatic lentiviral transgenesis and probed them by fluorescence calcium imaging. It turned out that lentivirus-driven *Foxg1* overexpression increased both discharge frequency and synchronization of these cultures (Fig. 6). As gabaergic neurons were ≤ 15% of total neurons, then the activity profiles displayed by these cultures should mainly represent the average behavior of their glutamatergic neurons. Consistently with our results, a reduced sensitivity to glutamate was recently reported in pyramidal neurons of *Foxg1*$^{+/-}$ mutants (in these mutants - however - the neocortex was globally more active, possibly reflecting decreased KCC2 and increased vGluT2 expression)[141]. Remarkably, this positive correlation between *Foxg1* expression levels and neuron excitability/activity is not restricted to glutamatergic neurons, but also seems to apply to gabaergic ones. Indeed, a decrease of discharge frequency upon current injection was documented in SST^{+} neocortical interneurons, upon selective *Foxg1* ablation in these cells [142], and a dramatic drop of gabaergic neuron discharge frequency was described in human telencephalic organoids where FOXG1 protein was artificially downregulated by up to -40% [143].

Concerning cellular origin of hyperactivity in our cultures, a positive correlation between *Foxg1* expression levels and neuron network *activity* emerged following both GOF and LOF *Foxg1* manipulations, provided that these manipulations included glutamatergic neurons. This suggests a pivotal causative role for these cells. However, the pronounced shrinkage of the interneuronal compartment elicited by generalized and pan-neuronal *Foxg1* upregulation did undoubtedly also contribute to such hyperactivity. As for neuronal hyper-synchronization, this phenomenon occurred only when *Foxg1* overexpressing cells included gabaergic neurons, pointing to mechanisms strictly requiring these cells.

Next, a pronounced shrinkage of the interneuronal compartment only took place when the over-expression of our *Foxg1* transgene was driven by promoters firing within GABA-ergic neurons (Fig. 7). Viceversa, no major drop of GABAergic-to-glutamatergic neuron ratio occurred when Foxg1 overexpression was confined to astrocytes or pyramidal neurons. This suggests that high *Foxg1* levels are cell-autonomously and selectively harmful to interneurons. Of note, dampening *Foxg1* by RNAi conversely elicited only a light decline of the GABAergic glutamatergic neuron prevalence

ratio, further suggesting that interneurons are resilient to moderate downward fluctuations *Foxg1* expression levels may physiologically undergo (Tigani, Pinzan et al., submitted). However, a more pronounced *Foxg1* downregulation can be seriously detrimental to these cells. Indeed, a drop of gabaergic interneuron prevalence was reported to occurr in human organoids upon pronounced and chronic FOXG1 knock-down (-70%) [143], and a specific decrease of SST+ inteneuron frequency was also documented in murine mutants lacking *Foxg1* in these cells [142].

Looking for underlying molecular mechanisms, we profiled the transcriptome of our engineered cultures. Results of this analysis included an upregulation of large Scn genes. Conversely, Scn1a, required for interneuron inhibitory activity, was decreased by about 4-folds. Cacn genesets, encoding for Na^+ and Ca^{2+} channels, were prevalently increased, pointing to a possible increase of Cacn-dependent Ca^{2+} currents. General dynamics of Scn and Cacn genes prefigure neuron hyperexcitability. Complex anomalies in other key genes governing Ca^{2+} fluxes, as well as aberrancies in Grin, Gria and Grik, NMDA, AMPA- and KA-receptor genes were reported. Genes encoding for ionotropic glutamatergic receptors showed a pattern definitively consistent with increased neocortical activity. Grik1 was downregulated; Grik3, encoding for the principal GluK3 subunit, was upregulated, Grik4 and Grik5, both essential for the normal ionotropic function, were increased as well. As for Gria family, both Gria2, decreasing Ca^{2+} permeability of AMPA receptors, and Gria4, needed to prevent epileptic seizures, were downregulated. Finally, concerning Grin genes, in addition to Grin1 decline, Grin2c/Grin2a and Grin2d/Grin2a ratios were dramatically upregulated, pointing to likely prolonged opening times of NMDA receptors. Grin3, normally limiting Ca2+ permeability of these receptors, was downregulated. Unbalanced expression of Gria, Grik and Grin genes might result into strengthened glutamatergic conduction. Moreover, a collapse of the GABAergic axis, including Gad1, Gad2, Gabra1 and Bdnf was reported and might jeopardize GABAergic control of neocortical circuits (Fig. 8).

Taken together, these data point out the crucial role of *Foxg1* expression in promoting neocortical electrical activity. We further wondered if culture hyperactivity, in turn, might stimulate Foxg1 expression. In fact, the resulting vicious circle might help us to explain the paroxysmal electrical activity described in patients affected by *FOXG1* duplications and West syndrome.

Previous experiment in our lab revealed that *Foxg1*-mRNA is transiently upregulated under high extracellular K^+ ions concentration, suggesting that its transcription is physiologically sensitive to changes of electric activity. Intriguingly, bioinformatic inspection of the Foxg1 locus revealed a

number of binding sites for immediate early genes (Fig. 10). This factors resulted necessary for *Foxg1*-mRNA increase, since their functional knock-down, generally reduced *Foxg1*-mRNA both in basal conditions and under high [K+]O (Tigani, Pinzan et al., submitted). As expected [131,144,145], some of them (or their mRNAs) showed a pronounced upregulation, which preceded the *Foxg1*-mRNA maximum at three hours. Specifically, pCreb1 and nuclear-Nfkb peaked at 20 min. *Cebpb*-mRNA level reaches the peak about an hour after the administration of KCl, consistently with other transcriptionally regulated IEGs previously monitored (*Fos, Egr1, Egr2*). All that points to an involvement of these effectors in mediating the impact of electric activity on *Foxg1* levels.

In summary, Foxg1 expression promotes neocortical electrical activity which, in turn, may stimulate Foxg1 expression. This feedback suggests a crucial role of *Foxg1* gene in fine tuning of neocortical excitability. In this respect, mis-regulation of *Foxg1*-mRNA in patients with *Foxg1* copy number variations might deeply affect neuronal activity, resulting in their Rett-like- and West-like EEG aberrancies [61,146]. Consistently, gentle stimulation of Foxg1 by saRNAs led to a complex upward distortion of fluctuations of pCreb1- and Nfkb-activity, as well as of Fos-, Egr1- (unpublished results) and Cebp-mRNAs, evoked by high [K+]O (Fig. 13). Prolonged upregulation of pCreb1, Egr1 and Fos may promote neuronal hyper-activity and -excitability [134–140,147–150] .

6. References

1. O'Leary, D. D. M., Chou, S. J. & Sahara, S. Area patterning of the mammalian cortex. *Neuron* **56**, 252–269 (2007).

2. Marin-Padilla, M. Early prenatal ontogenesis of the cerebral cortex (neocortex) of the cat (Felis domestica). A Golgi study - I. The primordial neocortical organization. *Z. Anat. Entwicklungsgesch.* **134**, 117–145 (1971).

3. Smart, I. H. M. Three dimensional growth of the mouse isocortex. *J. Anat.* **137**, 683–694 (1983).

4. Gillies, K. & Price, D. J. The Fates of Cells in the Developing Cerebral Cortex of Normal and Methylazoxymethanol Acetate-lesioned Mice. *Eur. J. Neurosci.* **5**, 73–84 (1993).

5. Price, D. J. & Willshaw, D. J. Mechanisms of Cortical Development. Chapter 2 - Early development of the telencephalon. in (2010).

6. Götz, M. & Huttner, W. B. The cell biology of neurogenesis. *Nat. Rev. Mol. Cell Biol.* **6**, 777–788 (2005).

7. Chenn, A. & McConnell, S. K. Cleavage orientation and the asymmetric inheritance of Notch1 immunoreactivity in mammalian neurogenesis. *Cell* **82**, 631–641 (1995).

8. Smart, I. H. Proliferative characteristics of the ependymal layer during the early development of the mouse neocortex: a pilot study based on recording the number, location and plane of cleavage of mitotic figures. *J. Anat.* **116**, 67–91 (1973).

9. Hartfuss, E., Galli, R., Heins, N. & Götz, M. Characterization of CNS precursor subtypes and radial glia. *Dev. Biol.* **229**, 15–30 (2001).

10. Malatesta, P. *et al.* Neuronal or glial progeny: Regional differences in radial glia fate. *Neuron* **37**, 751–764 (2003).

11. Rakic, P. Mode of cell migration to the superficial layers of fetal monkey neocortex. *J. Comp. Neurol.* **145**, 61–83 (1972).

12. Rakic, P. Developmental and evolutionary adaptations of cortical radial glia. *Cereb. Cortex* **13**, 541–549 (2003).

13. Noctor, S. C., Flint, A. C., Weissman, T. A., Dammerman, R. S. & Kriegstein, A. R. Neurons derived from radial glial cells establish radial units in neocortex. *Nature* **409**, 714–720 (2001).

14. Anthony, T. E., Klein, C., Fishell, G. & Heintz, N. Radial Glia Serve as Neuronal Progenitors in All Regions of the Central Nervous System has shown that they can be divided into multiple antigenically distinct subpopulations that differ in their cell cycle kinetics, with each subpopulation changing in a . *Neuron* **41**, 881–890 (2004).

15. Heins, N. *et al.* Glial cells generate neurons: The role of the transcription factor Pax6. *Nat. Neurosci.*

5, 308–315 (2002).

16. Malatesta, P., Hartfuss, E. & Götz, M. Isolation of radial glial cells by fluorescent-activated cell sorting reveals a neural lineage. *Development* **127**, 5253–5263 (2000).

17. Mo, Z. *et al.* Human cortical neurons originate from radial glia and neuron-restricted progenitors. *J. Neurosci.* **27**, 4132–4145 (2007).

18. Mallamaci, A. & Stoykova, A. Gene networks controlling early cerebral cortex arealization. *Eur. J. Neurosci.* **23**, 847–856 (2006).

19. Muzio, L. *et al.* Conversion of cerebral cortex into basal ganglia in Emx2−/− Pax6Sey/Sey double-mutant mice. *Nat. Neurosci.* **5**, 737–745 (2002).

20. Land, P. W. & Monaghan, A. P. Expression of the transcription factor, tailless, is required for formation of superficial cortical layers. *Cereb. Cortex* **13**, 921–931 (2003).

21. Roy, K. *et al.* The tlx gene regulates the timing of neurogenesis in the cortex. *J. Neurosci.* **24**, 8333–8345 (2004).

22. Estivill-Torrus, G., Pearson, H., van Heyningen, V., Price, D. J. & Rashbass, P. Pax6 is required to regulate the cell cycle and the rate of progression from symmetrical to asymmetrical division in mammalian cortical progenitors. *Development* **129**, 455–466 (2002).

23. Molyneaux, B. J., Arlotta, P., Menezes, J. R. L. & Macklis, J. D. Neuronal subtype specification in the cerebral cortex. *Nat. Rev. Neurosci.* **8**, 427–437 (2007).

24. Anderson, S. A. Distinct Origins of Neocortical Projection Neurons and Interneurons In Vivo. *Cereb. Cortex* **12**, 702–709 (2002).

25. Gorski, J. A. *et al.* Cortical excitatory neurons and glia, but not GABAergic neurons, are produced in the Emx1-expressing lineage. *J. Neurosci.* **22**, 6309–6314 (2002).

26. Tan, S. S. *et al.* Separate progenitors for radial and tangential cell dispersion during development of the cerebral neocortex. *Neuron* **21**, 295–304 (1998).

27. Ware, M. L., Tavazoie, S. F., Reid, C. B. & Walsh, C. A. Coexistence of widespread clones and large radial clones in early embryonic ferret cortex. *Cereb. Cortex* **9**, 636–645 (1999).

28. Noctor, S. C., Martinez-Cerdeño, V., Ivic, L. & Kriegstein, A. R. Cortical neurons arise in symmetric and asymmetric division zones and migrate through specific phases. *Nat. Neurosci.* **7**, 136–144 (2004).

29. LoTurco, J. J. & Bai, J. The multipolar stage and disruptions in neuronal migration. *Trends Neurosci.* **29**, 407–413 (2006).

30. Wonders, C. P. & Anderson, S. A. The origin and specification of cortical interneurons. *Nat. Rev. Neurosci.* **7**, 687–696 (2006).

31. Nadarajah, B. & Parnavelas, J. G. Modes of neuronal migration in the developing cerebral cortex. *Nat. Rev. Neurosci.* **3**, 423–432 (2002).

32. Miyoshi, G. & Fishell, G. GABAergic interneuron lineages selectively sort into specific cortical layers during early postnatal development. *Cereb. Cortex* **21**, 845–852 (2011).

33. O'Leary, D. D. M. & Terashima, T. Cortical axons branch to multiple subcortical targets by interstitial axon budding: Implications for target recognition and 'waiting periods'. *Neuron* **1**, 901–910 (1988).

34. O'Leary, D. D. M. & Koester, S. E. Development of projection neuron types, axon pathways, and patterned connections of the mammalian cortex. *Neuron* **10**, 991–1006 (1993).

35. Schreyer, D. & Jones, E. Axon elimination in the developing corticospinal tract of the rat. *Brain Res.* 103–19 (1988).

36. Arlotta, P. *et al.* Neuronal subtype-specific genes that control corticospinal motor neuron development in vivo. *Neuron* **45**, 207–221 (2005).

37. Inoue, K., Terashima, T., Nishikawa, T. & Takumi, T. Fez1 is layer-specifically expressed in the adult mouse neocortex. *Eur. J. Neurosci.* **20**, 2909–2916 (2004).

38. Molyneaux, B. J., Arlotta, P., Hirata, T., Hibi, M. & Macklis, J. D. Fezl is required for the birth and specification of corticospinal motor neurons. *Neuron* **47**, 817–831 (2005).

39. Chen, J. G., Rašin, M. R., Kwan, K. Y. & Šestan, N. Zfp312 is required for subcortical axonal projections and dendritic morphology of deep-layer pyramidal neurons of the cerebral cortex. *Proc. Natl. Acad. Sci. U. S. A.* **102**, 17792–17797 (2005).

40. Weimann, J. M. *et al.* Cortical neurons require Otx1 for the refinement of exuberant axonal projections to subcortical targets. *Neuron* **24**, 819–831 (1999).

41. Gray, P. A. *et al.* Mouse brain organization revealed through direct genome-scale TF expression analysis. *Science (80-.).* **306**, 2255–2257 (2004).

42. Lein, E. S. *et al.* Genome-wide atlas of gene expression in the adult mouse brain. *Nature* **445**, 168–176 (2007).

43. Magdaleno, S. *et al.* BGEM: An in situ hybridization database of gene expression in the embryonic and adult mouse nervous system. *PLoS Biol.* **4**, 497–500 (2006).

44. Visel, A. GenePaint.org: an atlas of gene expression patterns in the mouse embryo. *Nucleic Acids Res.* **32**, 552D–556 (2004).

45. Franco, S. *et al.* Fate-Restricted Neural Progenitors in the Mammalian Cerebral Cortex. *Science (80-.).* **337**, 746–749 (2012).

46. Guo, C. *et al.* Fezf2 expression identifies a multipotent progenitor for neocortical projection neurons, astrocytes and oligodendrocytes. *Neuron* (2013).

47. Ge, W.-P. & Jia, J.-M. Local production of astrocytes in the cerebral cortex. *Neuroscience* **176**, 3–9 (2016).

48. Rowitch, D. H. & Kriegstein, A. R. Developmental genetics of vertebrate glial-cell specification. *Nature* **468**, 214–222 (2010).

49. Sloan, S. & Barres, B. Mechanisms of astrocyte development and their contributions to neurodevelopmental disorders. *Curr. Opin. Neurobiol.* 75–81 (2014). doi:10.1111/mec.13536.Application

50. Privat, A., Gimenez-Ribotta, M. & Ridet, J.-C. Morphology of astrocytes. *Neuroglia* 3–22 (1995).

51. Arnold Kriegstein, A. & Alvarez-Buylla, A. The Glial Nature of Embryonic and Adult Neural Stem Cells. *Annu. Rev. Neurosci.* (2009).

52. Ge, W.-P., Miyawaki, A., Gage, F. H., Jan, Y. N. & Jan, Yeh, L. Local generation of glia is a major astrocyte source in postnatal cortex. *Nature* **484**, 376–380 (2013).

53. Hajós, F., Woodhams, P. L., Bascó, E., Csillag, A. & Balázs, R. Proliferation of astroglia in the embryonic mouse forebrain as revealed by simultaneous immunocytochemistry and autoradiography. *Acta Morphol. Acad. Sci. Hung.* **29**, 361—364 (1981).

54. Ichikawa, M., Shiga, T. & Hirata, Y. Spatial and temporal pattern of postnatal proliferation of glial cells in the parietal cortex of the rat. *Dev. Brain Res.* **9**, 181–187 (1983).

55. Bromfield, E., Cavazos, J. & Sirven, J. Basic Mechanisms Underlying Seizures and Epilepsy. in *An introduction to epilepsy* (2006).

56. Niciu, M. J., Kelmendi, B. & Sanacora, G. Overview of glutamatergic neurotransmission in the nervous system. *Pharmacol. Biochem. Behav.* **100**, 656–664 (2012).

57. Wu, C. & Sun, D. GABA receptors in brain development, function, and injury. *Metab. Brain Dis.* **30**, 367–379 (2015).

58. Fellin, T. & Carmignoto, G. Neurone-to-astrocyte signalling in the brain represents a distinct multifunctional unit. *J. Physiol.* **559**, 3–15 (2004).

59. Parri, H. R., Gould, T. M. & Crunelli, V. Spontaneous astrocytic Ca2+ oscillations in situ drive NMDAR-mediated neuronal excitation. *Nat. Neurosci.* **4**, 803–812 (2001).

60. Stafstrom, C. E. & Carmant, L. Seizures and epilepsy: An overview for neuroscientists. *Cold Spring Harb. Perspect. Biol.* **7**, 1–19 (2015).

61. Florian, C., Bahi-buisson, N. & Bienvenu, T. FOXG1 -Related Disorders: From Clinical Description to Molecular Genetics. *Mol. Syndromol.* **2**, 153–163 (2011).

62. Thomas, P. & Beddington, R. Anterior primitive endoderm may be responsible for patterning the anterior neural plate in the mouse embryo. *Curr. Biol.* **6**, 1487–1496 (1996).

63. Altmann, C. R. & Brivanlou, A. H. Neural patterning in the vertebrate embryo. *Int. Rev. Cytol.* **203**, 447–482 (2001).

64. Sasai, Y. & De Robertis, E. M. Ectodermal patterning in vertebrate embryos. *Dev. Biol.* **182**, 5–20 (1997).

65. Houart, C., Westerfield, M. & Wilson, S. W. A small population of anterior cells patterns the forebrain during zebrafish gastrulation. *Nature* **391**, 788–792 (1998).

66. Shimamura, K. & Rubenstein, J. L. R. Inductive interactions direct early regionalization of the mouse forebrain. *Development* **124**, 2709–2718 (1997).

67. Danesin, C. *et al.* Integration of Telencephalic Wnt and Hedgehog Signaling Center Activities by Foxg1. *Dev. Cell* **16**, 576–587 (2009).

68. Grove, E. A., Tole, S., Limon, J., Yip, L. W. & Ragsdale, C. W. The hem of the embryonic cerebral cortex is defined by the expression of multiple Wnt genes and is compromised in Gli3-deficient mice. *Development* **125**, 2315–2325 (1998).

69. Kuschel, S., Rüther, U. & Theil, T. A disrupted balance between Bmp/Wnt and Fgf signaling underlies the ventralization of the Gli3 mutant telencephalon. *Dev. Biol.* **260**, 484–495 (2003).

70. Rallu, M. *et al.* Dorsoventral patterning is established in the telencephalon of mutants lacking both Gli3 and hedgehog signaling. *Development* **129**, 4963–4974 (2002).

71. Xuan, S. *et al.* Winged helix transcription factor BF-1 is essential for the development of the cerebral hemispheres. *Neuron* **14**, 1141–1152 (1995).

72. Muzio, L., Soria, J. M., Pannese, M., Piccolo, S. & Mallamaci, A. A mutually stimulating loop involving Emx2 and canonical Wnt signalling specifically promotes expansion of occipital cortex and hippocampus. *Cereb. Cortex* **15**, 2021–2028 (2005).

73. Hanashima, C., Li, S. C., Shen, L., Lai, E. & Fishell, G. Foxg1 Suppresses Early Cortical Cell Fate. *Science (80-.).* **303**, 56–59 (2004).

74. Hanashima, C., Fernandes, M., Hebert, J. M. & Fishell, G. The role of Foxg1 and dorsal midline signaling in the generation of Cajal-Retzius subtypes. *J. Neurosci.* **27**, 11103–11111 (2007).

75. Takahashi, T. The Cell Cycle of the Pseudostratified Embryonic Murine Cerebral Wall. *J. Neurosci.* **15**, 6046–6057 (1995).

76. Calegari, F. & Huttner, W. B. An inhibition of cyclin-dependent kinases that lengthens, but does not arrest, neuroepithelial cell cycle induces premature neurogenesis. *J. Cell Sci.* **116**, 4947–4955 (2003).

77. Brancaccio, M., Pivetta, C., Granzotto, M., Filippis, C. & Mallamaci, A. Emx2 and Foxg1 inhibit gliogenesis and promote neuronogenesis. *Stem Cells* **28**, 1206–1218 (2010).

78. Hanashima, C., Shen, L., Li, S. C. & Lai, E. Brain factor-1 controls the proliferation and differentiation of neocortical progenitor cells through independent mechanisms. *J. Neurosci.* **22**, 6526–6536 (2002).

79. Martynoga, B., Morrison, H., Price, D. J. & Mason, J. O. Foxg1 is required for specification of ventral telencephalon and region-specific regulation of dorsal telencephalic precursor proliferation and apoptosis. *Dev. Biol.* **283**, 113–127 (2005).

80. Dou, C. L., Li, S. & Lai, E. Dual role of brain factor-1 in regulating growth and patterning of the cerebral hemispheres. *Cereb. Cortex* **9**, 543–550 (1999).

81. Seoane, J., Le, H.-V., Shen, L., Anderson, S. A. & Massague´, J. Integration of Smad and Forkhead Pathways in the Control of Neuroepithelial and Glioblastoma Cell Proliferation. *Cell* **117**, 211–223

(2004).

82. Fasano, C. A. *et al.* Bmi-1 cooperates with Foxgl to maintain neural stem cell self-renewal in the forebrain. *Genes Dev.* **23**, 561–574 (2009).

83. Barnes, A. P. *et al.* LKB1 and SAD Kinases Define a Pathway Required for the Polarization of Cortical Neurons. *Cell* **129**, 549–563 (2007).

84. Miyoshi, G. & Fishell, G. Dynamic FoxG1 Expression Coordinates the Integration of Multipolar Pyramidal Neuron Precursors into the Cortical Plate. *Neuron* **74**, 1045–1058 (2012).

85. Kumamoto, T. *et al.* Foxg1 Coordinates the Switch from Non-Radially to Radially Migrating Glutamatergic Subtypes in the Neocortex through Spatiotemporal Repression. *Cell Rep.* (2013).

86. Toma, K., Kumamoto, T., Hanashima, C., Toma, K. & Hanashima, C. The timing of upper-layer neurogenesis is conferred by sequential derepression and negative feedback from deep-layer neurons. *J. Neurosci.* **34**, 13259–13276 (2014).

87. Hou, P.-S., Miyoshi, G. & Hanashima, C. Sensory cortex wiring requires preselection of short- and long-range projection neurons through an Egr-Foxg1-COUP-TFI network. *Nat. Commun.* **10**, 1–18 (2019).

88. Pancrazi, L. *et al.* Foxg1 localizes to mitochondria and coordinates cell differentiation and bioenergetics. *Proc. Natl. Acad. Sci. U. S. A.* **112**, 13910–13915 (2015).

89. Chiola, S., Do, M. D., Centrone, L. & Mallamaci, A. Foxg1 overexpression in neocortical pyramids stimulates dendrite elongation via hes1 and pCreb1 upregulation. *Cereb. Cortex* **29**, 1006–1019 (2018).

90. Falcone, C. *et al.* Foxg1 Antagonizes Neocortical Stem Cell Progression to Astrogenesis . *Cereb. Cortex* 1–16 (2019). doi:10.1093/cercor/bhz031

91. Bhat, K. M., Van Beers, E. H. & Bhat, P. Sloppy paired acts as the downstream target of Wingless in the Drosophila CNS and interaction between sloppy paired and gooseberry inhibits sloppy paired during neurogenesis. *Development* **127**, 655–665 (2000).

92. MONDAL, S., IVANCHUK, S. M., RUTKA, J. T. & BOULIANNE, G. L. Sloppy Paired 1/2 Regulate Glial Cell Fates by Inhibiting Gcm Function. *Glia* 282–293 (2007).

93. Vegas, N. *et al.* Delineating FOXG1 syndrome: From congenital microcephaly to hyperkinetic encephalopathy. *Neurol. Genet.* **4**, (2018).

94. Mitter, D. *et al.* FOXG1 syndrome: Genotype-phenotype association in 83 patients with FOXG1 variants. *Genet. Med.* **20**, 98–108 (2018).

95. Tohyama, J. *et al.* West syndrome associated with mosaic duplication of FOXG1 in a patient with maternal uniparental disomy of chromosome 14. *Am. J. Med. Genet. Part A* **155**, 2584–2588 (2011).

96. Brunetti-Pierri, N. *et al.* Duplications of FOXG1 in 14q12 are associated with developmental epilepsy, mental retardation, and severe speech impairment. *Eur. J. Hum. Genet.* **19**, 102–107 (2011).

97. Pontrelli, G. *et al.* Epilepsy in patients with duplications of chromosome 14 harboring FOXG1. *Pediatr. Neurol.* **50**, 530–535 (2014).

98. Yeung, A. *et al.* 4.45 Mb microduplication in chromosome band 14q12 including FOXG1 in a girl with refractory epilepsy and intellectual impairment. *Eur. J. Med. Genet.* **52**, 440–442 (2009).

99. Striano, P. *et al.* WEST SYNDROME ASSOCIATED WITH 14q12 DUPLICATIONS HARBORING FOXG1. *Neurology* (2011).

100. Taghdiri, M. M. & Nemati, H. Infantile Spasm: A review article. *Iran. J. Child Neurol.* **8**, 1–5 (2014).

101. Bosi, S. *et al.* From 2D to 3D: Novel nanostructured scaffolds to investigate signalling in reconstructed neuronal networks. *Sci. Rep.* **5**, 1–11 (2015).

102. Rauti, R. *et al.* Graphene Oxide Nanosheets Reshape Synaptic Function in Cultured Brain Networks. *ACS Nano* **10**, 4459–4471 (2016).

103. Follenzi, A. & Naldini, L. Generation of HIV-1 derived lentiviral vectors. *Methods Enzymol. - Gene Ther. Issue* 454–465 (2002).

104. Tamamaki, N. *et al.* Green Fluorescent Protein Expression and Colocalization with Calretinin, Parvalbumin, and Somatostatin in the GAD67-GFP Knock-In Mouse. *J. Comp. Neurol.* **467**, 60–79 (2003).

105. Muzio, L. & Mallamaci, A. Foxg1 confines Cajal-Retzius neuronogenesis and hippocampal morphogenesis to the dorsomedial pallium. *J. Neurosci.* **25**, 4435–4441 (2005).

106. Catterall, W. A., Goldin, A. L. & Waxman, S. G. Nomenclature and structure-function relationships of voltage-gated sodium channels. *Pharmacol. Rev.* **57**, 397–409 (2005).

107. Johnston, J., Forsythe, I. D. & Kopp-Scheinpflug, C. Going native: Voltage-gated potassium channels controlling neuronal excitability. *J. Physiol.* **588**, 3187–3200 (2010).

108. Shah, N. H. & Aizenman, E. Voltage-Gated Potassium Channels at the Crossroads of Neuronal Function, Ischemic Tolerance, and Neurodegeneration. *Transl. Stroke Res.* **5**, 38–58 (2014).

109. Zamponi, G. W., Lory, P. & Perez-Reyes, E. Role of voltage-gated calcium channels in epilepsy. *Eur. J. Physiol.* (2009).

110. Kwon, S. K., Hirabayashi, Y. & Polleux, F. Organelle-specific sensors for monitoring Ca2+ dynamics in neurons. *Front. Synaptic Neurosci.* **8**, 1–9 (2016).

111. Raffaello, A., Mammucari, C., Gherardi, G. & Rizzuto, R. Calcium at the Center of Cell Signaling: Interplay between Endoplasmic Reticulum, Mitochondria, and Lysosomes. *Trends Biochem. Sci.* **41**, 1035–1049 (2016).

112. Traynelis, S. *et al.* Glutamate Receptor Ion Channels: Structure, Regulation, and Function. *Pharmacol. Rev.* **62**, 405–496 (2010).

113. Jembrek, Jazvinscak Maja Vlainic, J. GABA Receptors: Pharmacological Potential and Pitfalls. *Curr. Pharm. Des.* **21**, (2015).

114. Crupi, R., Impellizzeri, D. & Cuzzocrea, S. Role of metabotropic glutamate receptors in neurological disorders. *Front. Mol. Neurosci.* **12**, 1–11 (2019).

115. Gu, Q. Neuromodulatory transmitter systems in the cortex and their role in cortical plasticity. *Neuroscience* **111**, 815–835 (2002).

116. Monteiro, P. & Feng, G. SHANK proteins: Roles at the synapse and in autism spectrum disorder. *Nat. Rev. Neurosci.* **18**, 147–157 (2017).

117. Sun, Y. *et al.* A deleterious Nav1.1 mutation selectively impairs telencephalic inhibitory neurons derived from Dravet Syndrome patients. *Elife* **5**, 1–26 (2016).

118. Clayton, G. H., Owens, G. C., Wolff, J. S. & Smith, R. L. Ontogeny of cation-Cl- cotransporter expression in rat neocortex. *Dev. Brain Res.* **109**, 281–292 (1998).

119. Rivera, C. *et al.* The K+/Cl- co-transporter KCC2 renders GABA hyperpolarizing during neuronal maturation. *Nature* **397**, 251–255 (1999).

120. Dolphin, A. C. Voltage-gated calcium channels and their auxiliary subunits: physiology and pathophysiology and pharmacology. *J. Physiol.* **594**, 5369–5390 (2016).

121. Paternain, A. V., Cohen, A., Stern-Bach, Y. & Lerma, J. A role for extracellular Na+ in the channel gating of native and recombinant kainate receptors. *J. Neurosci.* **23**, 8641–8648 (2003).

122. Wisden, W. & Seeburg, P. H. A complex mosaic of high-affinity kainate receptors in rat brain. *J. Neurosci.* **13**, 3582–3598 (1993).

123. Fernandes, H. B. *et al.* High affinity kainate receptor subunits are necessary for ionotropic but not metabotropic signaling. *Neuron* **63**, 818–829 (2009).

124. Sanchez, R. M. *et al.* Decreased glutamate receptor 2 expression and enhanced epileptogenesis in immature rat hippocampus after perinatal hypoxia-induced seizures. *J. Neurosci.* **21**, 8154–8163 (2001).

125. Beyer, B. *et al.* Absence seizures in C3H/HeJ and knockout mice caused by mutation of the AMPA receptor subunit Gria4. *Hum. Mol. Genet.* **17**, 1738–1749 (2008).

126. Paoletti, P., Bellone, C. & Zhou, Q. NMDA receptor subunit diversity: Impact on receptor properties, synaptic plasticity and disease. *Nat. Rev. Neurosci.* **14**, 383–400 (2013).

127. Wada, A., Takahashi, H., Lipton, S. A. & Chen, H. S. V. NR3A modulates the outer vestibule of the 'NMDA' receptor channel. *J. Neurosci.* **26**, 13156–13166 (2006).

128. Hong, E. J., Mccord, A. E. & Greenberg, M. E. A biological function for the neuronal activity-dependent component of Bdnf transcription in the development of cortical inhibition. **60**, 610–624 (2010).

129. He, X. B. *et al.* Prolonged membrane depolarization enhances midbrain dopamine neuron differentiation via epigenetic histone modifications. *Stem Cells* **29**, 1861–1873 (2011).

130. Mathelier, A. *et al.* JASPAR 2014: An extensively expanded and updated open-access database of transcription factor binding profiles. *Nucleic Acids Res.* **42**, 142–147 (2014).

131. Flavell, S. W. & Greenberg, M. E. Expression and Plasticity of the Nervous System. *Annu Rev Neurosci* 563–590 (2008). doi:10.1146/annurev.neuro.31.060407.125631.Signaling

132. de la Torre-Ubieta, L. & Bonni, A. Transcriptional Regulation of Neuronal Polarity and Morphogenesis in the Mammalian Brain. *Neuron* **72**, 22–40 (2011).

133. Fimiani, C., Goina, E., Su, Q., Gao, G. & Mallamaci, A. RNA activation of haploinsufficient Foxg1 gene in murine neocortex. *Sci. Rep.* **6**, 1–13 (2016).

134. Jones, M. W., Errington, M. L. & French, P. J. A requirement for the immediate early gene Zif268 in the expression of late LTP and long-term memories. *Nat. Neurosci.* **4**, 289–96 (2001).

135. De Armentia, M. L. *et al.* cAMP response element-binding protein-mediated gene expression increases the intrinsic excitability of CA1 pyramidal neurons. *J. Neurosci.* **27**, 13909–13918 (2007).

136. Jancic, D., Lopez De Armentia, M., Valor, L. M., Olivares, R. & Barco, A. Inhibition of cAMP response element-binding protein reduces neuronal excitability and plasticity, and triggers neurodegeneration. *Cereb. Cortex* **19**, 2535–2547 (2009).

137. Viosca, J., De Armentia, M. L., Jancic, D. & Barco, A. Enhanced CREB-dependent gene expression increases the excitability of neurons in the basal amygdala and primes the consolidation of contextual and cued fear memory. *Learn. Mem.* **16**, 193–197 (2009).

138. Gruart, A., Benito, E., Delgado-García, J. M. & Barco, A. Enhanced cAMP response element-binding protein activity increases neuronal excitability, hippocampal long-term potentiation, and classical eyeblink conditioning in alert behaving mice. *J. Neurosci.* **32**, 17431–17441 (2012).

139. Penke, Z. *et al.* Zif268/Egr1 gain of function facilitates hippocampal synaptic plasticity and long-term spatial recognition memory. *Philos. Trans. R. Soc. B Biol. Sci.* **369**, 1–9 (2014).

140. Koldamova, R. *et al.* Genome-wide approaches reveal EGR1-controlled regulatory networks associated with neurodegeneration. *Neurobiol. Dis.* **63**, 107–114 (2014).

141. Testa, G. *et al.* Cortical Seizures in FoxG1+/− Mice are Accompanied by Akt/S6 Overactivation, Excitation/Inhibition Imbalance and Impaired Synaptic Transmission. *Int. J. Mol. Sci.* **20**, 4127 (2019).

142. Chen, D. *et al.* Loss of Foxg1 Impairs the Development of Cortical SST-Interneurons Leading to Abnormal Emotional and Social Behaviors. *Cereb. Cortex* **29**, 3666–3682 (2019).

143. Zhu, W. *et al.* Precisely controlling endogenous protein dosage in hPSCs and derivatives to model FOXG1 syndrome. *Nat. Commun.* **10**, (2019).

144. Calella, A. M. *et al.* Neurotrophin/Trk receptor signaling mediates C/EBPα, -β and NeuroD recruitment to immediate-early gene promoters in neuronal cells and requires C/EBPs to induce immediate-early gene transcription. *Neural Dev.* **2**, (2007).

145. Snow, W. M. & Albensi, B. C. Neuronal gene targets of NF-κB and their dysregulation in alzheimer's disease. *Front. Mol. Neurosci.* **9**, 1–19 (2016).

146. Seltzer, L. *et al.* Epilepsy and outcome in FOXG1 -related disorders. *Epilepsia* 1292–1300 (2014).

147. Zhou, Y. *et al.* CREB regulates excitability and the allocation of memory to subsets of neurons in the amygdala. *Nat. Neurosci.* **12**, 1438–1443 (2009).

148. Yassin, L. *et al.* An Embedded Subnetwork of Highly Active Neurons in the Neocortex. *Neuron* **68**, 1043–1050 (2010).

149. Descalzi, G. *et al.* Rapid synaptic potentiation within the anterior cingulate cortex mediates trace fear learning. *Mol. Brain* **5**, 1–14 (2012).

150. Ryan, T. J., Roy, D. S., Pignatelli, M., Arons, A. & Tonegawa, S. Engram cells retain memory under retrograde amnesia. *Science (80-.).* **348**, 1007–1013 (2015).

Acknowledgement

Lot of people contributed to this work and deserve my sincere gratitude.

Thanks to Moira Pinzan for sharing this project with me. She layed the foundation of my work characterizing Foxg1 GOF model and carrying out the first experiments on Foxg1 response to electric activity and IEGs.

Thanks to Osvaldo Artimagnella for sharing the results from RNA sequencing of Foxg1 GOF neurons and for elucidating the dynamic of Foxg1 protein upon electric activity.

Thanks to Manuela Santo for helping me with Ca2+ imaging experiments.

Thanks to my collaborators who performed Ca2+ imaging recordings: Teresa Sorbo and Rossana Rauti from Prof. Ballerini group and Francesco Ulloa from Prof. Torre group. They allowed us to deepen this study with their expertise, availability and advices.

Thanks to Simone Mortal for his tireless patience, constant support and incomparable microscopy skills. For being close whether I deserved it or not.

Thanks to Lorenzo Fant. For forcing me to start writing this work. For dragging me where everything looks small and far, away from all of my concerns.

Thanks to Giovanni Antonio Piredda, for turning a new place into home. I would be starving without you.

Thanks to my labmates, both present and former members of the group. Thank you for being friends before than colleagues, my inexhaustible source of laugh, fight, hugs, LV aliquots and leftover cells. I know I could not have asked for better people around me during these years. How could I do this without you?